

# Geochemistry, Geophysics, Geosystems

## RESEARCH ARTICLE

10.1029/2020GC009219

### Special Section:

Magmatic and Volcanic Processes in Continental Rifts

### Key Points:

- The first published event tree model to quantify volcanic hazard at an African volcano is presented for Aluto (Ethiopia)
- The event tree facilitates the design of a conceptual model for Aluto and provides a framework to quantify volcanic hazard
- The impact of epistemic uncertainty is explored by merging diverse data sets, from field data to expert elicitation and global databases

### Supporting Information:

- Supporting Information S1
- Figure S1
- Data Set S1
- Data Set S2
- Data Set S3
- Data Set S4
- Data Set S5

### Correspondence to:

P. Tierz,  
pablo@bgs.ac.uk

### Citation:

Tierz, P., Clarke, B., Calder, E. S., Dessalegn, F., Lewi, E., Yirgu, G., et al. (2020). Event trees and epistemic uncertainty in long-term volcanic hazard assessment of rift volcanoes: The example of Aluto (Central Ethiopia). *Geochemistry, Geophysics, Geosystems*, 21, e2020GC009219. <https://doi.org/10.1029/2020GC009219>

Received 5 JUN 2020

Accepted 14 AUG 2020

Accepted article online 20 AUG 2020

©2020. United Kingdom Research and Innovation.

This is an open access article under the terms of the Creative Commons Attribution License, which permits use, distribution and reproduction in any medium, provided the original work is properly cited.

## Event Trees and Epistemic Uncertainty in Long-Term Volcanic Hazard Assessment of Rift Volcanoes: The Example of Aluto (Central Ethiopia)

P. Tierz<sup>1,2</sup> , B. Clarke<sup>2,3</sup> , E. S. Calder<sup>2</sup>, F. Dessalegn<sup>4</sup>, E. Lewi<sup>5</sup> , G. Yirgu<sup>6</sup>, K. Fontijn<sup>7</sup> , J. M. Crummy<sup>1</sup>, Y. Bekele<sup>8</sup>, and S. C. Loughlin<sup>1</sup>

<sup>1</sup>British Geological Survey, The Lyell Centre, Edinburgh, UK, <sup>2</sup>School of Geosciences, University of Edinburgh, Edinburgh, UK, <sup>3</sup>School of Geography, Geology and the Environment, University of Leicester, Leicester, UK, <sup>4</sup>CNCS, Wollega University, Nekemte, Ethiopia, <sup>5</sup>Institute of Geophysics, Space Science and Astronomy, Addis Ababa University, Addis Ababa, Ethiopia, <sup>6</sup>School of Earth Sciences, Addis Ababa University, Addis Ababa, Ethiopia, <sup>7</sup>Department of Geosciences, Environment and Society, Université Libre de Bruxelles, Brussels, Belgium, <sup>8</sup>Geo-hazard Investigation Directorate, Geological Survey of Ethiopia, Addis Ababa, Ethiopia

**Abstract** Aluto is a peralkaline rhyolitic caldera located in a highly populated area in central Ethiopia. Its postcaldera eruptive activity has mainly consisted of self-similar, pumice-cone-building eruptions of varying size and vent location. These eruptions are explosive, generating hazardous phenomena that could impact proximal to distal areas from the vent. Volcanic hazard assessments in Ethiopia and the East African Rift are still limited in number. In this study, we develop an event tree model for Aluto volcano. The event tree is doubly useful: It facilitates the design of a conceptual model for the volcano and provides a framework to quantify volcanic hazard. We combine volcanological data from past and recent research at Aluto, and from a tool to objectively derive analog volcanoes (VOLCANS), to parameterize the event tree, including estimates of the substantial epistemic uncertainty. Results indicate that the probability of a silicic eruption in the next 50 years is highly uncertain, ranging from 2% to 35%. This epistemic uncertainty has a critical influence on event-tree estimates for other volcanic events, like the probability of occurrence of pyroclastic density currents (PDCs) in the next 50 years. The 90% credible interval for the latter is 5–16%, considering only the epistemic uncertainty in conditional eruption size and PDC occurrence, but 2–23% when adding the epistemic uncertainty in the probability of eruption in 50 years. Despite some anticipated challenges, we envisage that our event tree could be translated to other rift volcanoes, making it an important tool to quantify volcanic hazard in Ethiopia and elsewhere.

## 1. Introduction

Active volcanoes have the potential to cause extreme losses in terms of fatalities and casualties, damage to property and critical infrastructure, and due to disruption of transport and supply chains (e.g., Auker et al., 2013; Blong, 1984; Brown et al., 2017; Horwell & Baxter, 2006; Loughlin et al., 2015; Newhall et al., 2018; Wilson et al., 2012). Therefore, quantifying volcanic hazard is a priority for the volcanological community, and methods have increasingly been developed over recent decades (e.g., Aspinall et al., 2003; Bayarri et al., 2009; Bebbington, 2013, 2014, 2015; Bevilacqua et al., 2016, 2017; Connor et al., 2001, 2012; Hincks et al., 2014; Jenkins et al., 2012; Marzocchi et al., 2004, 2008, 2010; Newhall & Hoblitt, 2002; Sandri et al., 2012, 2018; Selva et al., 2014; Tierz et al., 2017; and many others, cf. Connor et al., 2015; Marzocchi & Bebbington, 2012; Poland & Anderson, 2020; Tierz, 2020). Volcanic hazard quantification is particularly urgent in Africa, where data scarcity and infrequent eruptions pose particular challenges.

Ethiopia is the second most populous nation (estimated ~110 million inhabitants; e.g., World Bank, World Development Indicators, 2019) and the fastest growing economy in Africa (World Bank, <https://data.worldbank.org/region/sub-saharan-africa>). Ethiopia also holds the largest number of Holocene volcanoes (~60) in the African continent (e.g., Global Volcanism Program, 2013). Globally, Ethiopia ranks second only to Indonesia in having the largest number of active volcanoes at the highest level of uncertainty related to volcanic hazard (i.e., in terms of available data and monitoring activities, Aspinall et al., 2011). Additionally, exposure to volcanic hazard is high in Ethiopia (Aspinall et al., 2011) and is rapidly increasing with continued economic and industrial development (Aspinall et al., 2011; United Nations

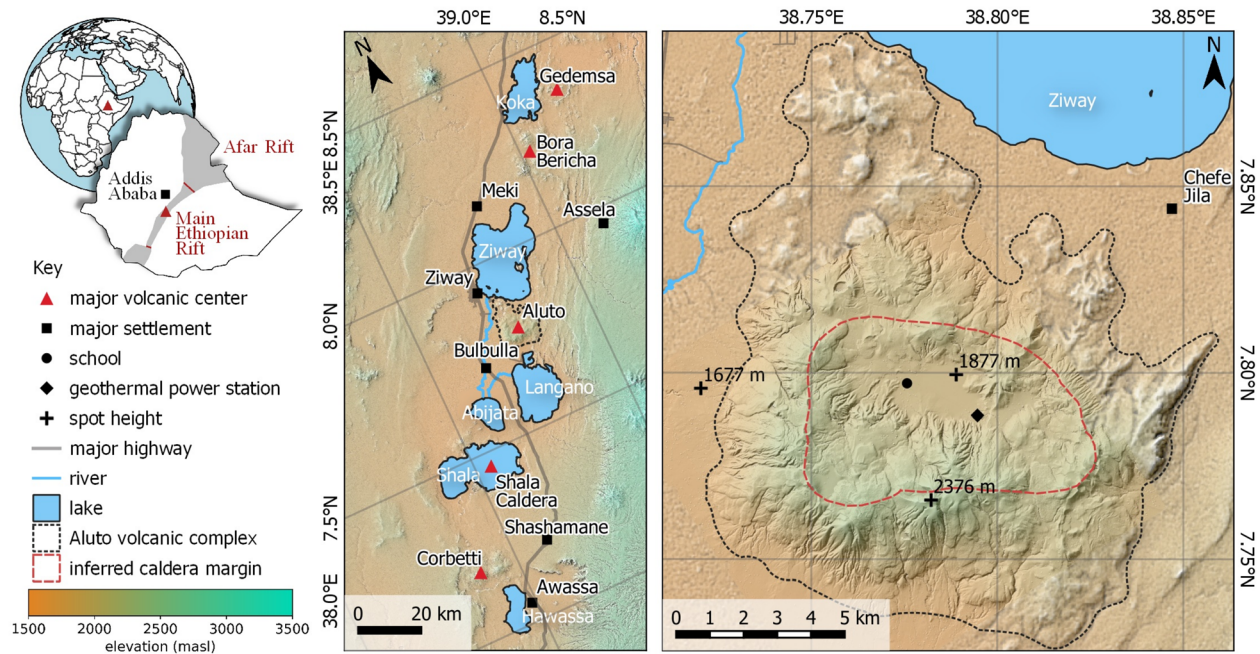


**Figure 1.** Geographic and simplified volcanologic setting for Aluto volcano, in the Main Ethiopian rift. Adapted from Clarke et al. (2020). [Modifications © BGS-UKRI. Modified after © 2020 Clarke et al. Creative Commons Attribution License (CC BY)].

Development Programme, 2018; Vye-Brown et al., 2016). Despite this, contributions to volcanic hazard assessment in the East African Rift System (EARS) have been limited and are inevitably based on very little data. They have consisted of preliminary regional volcanic hazard assessments (e.g., Aspinall et al., 2011; Jenkins et al., 2015) alongside some overview contributions (e.g., Vye-Brown et al., 2016; Yirgu et al., 2014). Volcanological knowledge and supporting data sets are increasing in the form of: geological maps, regional and local pyroclastic stratigraphies, physical interpretations of volcanic processes, radiometric dates, and geochemical analyses (Clarke, 2020; Clarke et al., 2019; Fontijn et al., 2010, 2011, 2012, 2018; Hunt et al., 2019; Hutchison, Pyle, et al., 2016; Hutchison et al., 2018; Iddon et al., 2019; Martin-Jones et al., 2017; McNamara et al., 2018; Rapprich et al., 2016). The collection and compilation of such volcanological data sets are of paramount importance to quantify volcanic hazard (e.g., Tierz, 2020) and also to underpin the design and implementation of volcano disaster risk reduction strategies in Ethiopia and the wider East African region.

Aluto is a volcanic system in the central Main Ethiopian Rift (MER, Figure 1), which has recently shown signs of volcanic unrest, as recorded by ground deformation, gas emissions, and seismic data (Biggs et al., 2011; Hutchison et al., 2015; Hutchison, Biggs, et al., 2016; Wilks et al., 2017). There have been no observed or documented historical eruptions. The volcano is located between the shallow Lake Ziway to the north (2.5 m average-depth, Hengsdijk & Jansen, 2006), Lake Langanu to the south and East Ziway (e.g., Hunt et al., 2020), a basaltic volcanic field with an unestablished relation to the Aluto volcanic system (e.g., Fontijn et al., 2018; Hutchison, Pyle, et al., 2016), to the northeast. An estimated 200–300k people live within a radius of approximately 20 km from the center of Aluto caldera (Clarke, 2020; Vye-Brown et al., 2016, and references therein). The caldera floor itself hosts numerous rural villages/settlements, a school, and the Aluto-Langanu geothermal power station. The *woredas* (districts) of Ziway town (now called Batu, ~44k inhabitants, Central Statistical Agency, 2007) and Adami Tullu/Jido Kombolcha (~141k inhabitants, Central Statistical Agency, 2007) are located to the NW, W, and SW of the volcano.

Even though many questions still remain about the eruptive history of Aluto volcano (e.g., frequency-magnitude distributions), it is to date one of the best studied/well-known volcanoes across the entire EARS. In this work, we collect the existing volcanological knowledge on the Aluto volcanic system and its potential eruptive behavior (much of which was acquired over the last decade) and use it to inform an assessment

of the long-term volcanic hazard associated with future eruptions at the volcano, including the significant uncertainties involved. The assessment presented in this work is meant to act as a framework to quantify volcanic hazard at Aluto and not as a comprehensive, full volcanic hazard assessment of all its possible hazardous phenomena before, during and after a future eruption.

We use an event tree model (Newhall & Hoblitt, 2002), which is a probabilistic graphical model (Koller & Friedman, 2009) that encodes our understanding of how a given volcanic system functions (e.g., Newhall & Pallister, 2015). This represents one approach to model the joint probability distribution of eruption onset, location, size, and style, including the occurrence of different volcanic hazardous phenomena, such as tephra fallout, pyroclastic density currents (PDCs), or lava flows (e.g., Marzocchi et al., 2004, 2008, 2010; Neri et al., 2008; Newhall & Hoblitt, 2002; Newhall & Pallister, 2015; Sandri et al., 2012, 2014, 2018; Sobradelo et al., 2014; Sobradelo & Martí, 2010; Tierz et al., 2018; Tonini et al., 2015; Wright et al., 2019). Hence, event trees are used to capture this natural variability in volcanic activity, or aleatory uncertainty, which is the primary source of uncertainty in probabilistic volcanic hazard assessment, PVHA (e.g., Marzocchi et al., 2004; Tierz et al., 2018; Woo, 1999). Additionally, event trees can also be designed to incorporate and model the epistemic uncertainty, which is related to a lack of or incomplete knowledge, in order to derive comprehensive PVHA (e.g., Marzocchi et al., 2004, 2008, 2010). Epistemic uncertainty has been increasingly recognized as an important component of PVHA (e.g., Bebbington, 2013, 2014; Bevilacqua et al., 2015, 2016, 2017; Hincks et al., 2014; Rutarindwa et al., 2019; Sandri et al., 2014, 2018; Selva et al., 2018; Selva, Orsi, et al., 2012; Spiller et al., 2014; Stefanescu et al., 2012; Tierz et al., 2016). Epistemic uncertainty in event tree models is seldom quantified explicitly using probability estimations coming from different alternative data sets or models (e.g., Sandri et al., 2018). Commonly, it is subjectively assigned depending on the confidence or reliability on the data available or the hazard modeling setup (Sandri et al., 2012, 2014; Selva et al., 2010; Sobradelo & Martí, 2010; Tierz et al., 2018). It has also been estimated via expert elicitation (e.g., Neri et al., 2008; Queiroz et al., 2008). In some more sophisticated approaches, it has been quantified through model ensembles that integrate alternative assumptions on volcanological parameters such as the grain size distribution, particle aggregation, or column-collapse height (e.g., Sandri et al., 2018; Selva et al., 2018). Here, we present a parameterization of the event tree model that accounts for epistemic uncertainty by explicitly fitting probability density functions to alternative estimates of the frequency of different events across the model, expanding the approach of Sandri et al. (2018). This method allows us to incorporate varied data from recent research carried out at Aluto volcano into our PVHA. In particular, we use data coming from (1) proximal and distal volcanic deposits, (2) expert elicitation, and (3) sets of analog volcanoes identified using the VOLCano ANalogues Search tool (VOLCANS, Tierz et al., 2019). All the hazard estimates obtained through these data sets have been incorporated into our analysis and modeled homogeneously across the event tree model presented here.

In section 2, we summarize how past and present research has shaped the current volcanological knowledge available for Aluto. In section 3, we describe how this critical volcanological knowledge is used to build and parametrize an event tree model for Aluto, which serves as a conceptual model of the volcano as well as a framework to quantify its associated volcanic hazard. In section 4, we present some illustrative results of probabilistic assessments that can be derived from the model, including the effect of incorporating epistemic uncertainty on different nodes of the event tree. Finally, in section 5, we discuss the implications of our findings for PVHA at Aluto volcano and the challenges and opportunities to apply some of the approaches presented here to other volcanoes across the MER and the EARS.

## 2. Past and Present Volcanological Knowledge at Aluto

### 2.1. Regional Geological Context

The Main Ethiopian Rift is a mature continental rift sector within the Eastern branch of the East African Rift System (EARS, Figure 1). It stretches for over 500 km NE–SW in central Ethiopia, between the Afar triangle to the north and the tectonic transition between the Kenya and Ethiopian rifts to the south (e.g., Chorowicz, 2005; Corti, 2009; Ebinger, 2005; Mohr, 1983; Wadge et al., 2016; Woldegabriel et al., 1990). Aluto volcano is located in the central MER, the least mature portion of the MER, far younger (~5–6 Ma) than the southern and northern MER (~18–11 Ma) (Figure 1; Corti, 2009; Keranen & Klemperer, 2008). Continental rifting is commonly described as initiating on thick, cold, and predeformed continental

lithosphere and evolving through progressive crustal thinning, heating (by magma intrusion), and increasingly localized deformation, potentially culminating in the formation of new oceanic lithosphere (e.g., Corti, 2009, 2012; Ebinger, 2005). Being the youngest sector of the EARS in Ethiopia, the central MER has a thicker (up to 40 km), less-deformed upper crust and is dominated by large silicic calderas, such as Aluto, rather than by the basaltic volcanic systems that dominate the Afar rift to the north (e.g., Corti, 2009; Fontijn et al., 2018; Hutchison et al., 2018; Kendall et al., 2005; Lahitte et al., 2003).

Magmas in the MER are generated by decompression-driven (e.g., Rychert et al., 2012), low-degree partial mantle melting (Ebinger, 2005), with extensive fractional crystallization and minimal crustal assimilation (e.g., Gleeson et al., 2017; Hutchison et al., 2018). This results in bimodal alkaline basalt and peralkaline rhyolite erupted compositions (Barberi et al., 1974; Field et al., 2012; Hutchison, Pyle, et al., 2016; Iddon et al., 2019; Peccerillo et al., 2003, 2007; Rooney et al., 2012). Due to an excess of alkalis, which increases the proportion of nonbridging oxygens in the silica network, peralkaline rhyolites possess a relatively low viscosity in comparison to nonperalkaline magmas with similar silica contents (Baasner et al., 2013; Di Genova et al., 2013; Dingwell et al., 1998; Hess et al., 1995). Thus, at their respective eruption temperatures, hydrous peralkaline rhyolites show viscosities similar to basalts, and even when they are dry, their viscosity is around two orders of magnitude lower than a metaluminous rhyolite (Clarke et al., 2019; Di Genova et al., 2013; Dingwell et al., 1998). An eruption of peralkaline rhyolite magma has never been observed worldwide (e.g., Clarke et al., 2019), so our understanding of the nature of these eruptions relies solely on the geological record. Known peralkaline rhyolite eruptions in the geological record that did not form calderas mostly produced pumice cones (e.g., Clarke et al., 2019; Fontijn et al., 2018; Houghton et al., 1985; Orsi et al., 1989). Interpretations of the eruption styles that have led to the creation of pumice cones on Pantelleria (Italy) and Tuhua/Mayor Island (New Zealand) have been in part based on their resemblance to basaltic scoria cones, suggesting low explosivity (possibly prolonged) Hawaiian to Strombolian eruption styles (Houghton et al., 1985; Orsi et al., 1989). However, interpretations from recent studies in the MER indicate that pumice cones in Ethiopia may have been generated by moderate to large explosive eruptions, which generated convective eruption columns, relatively widespread tephra fall, and PDCs (Clarke, 2020; Clarke et al., 2019; Fontijn et al., 2018; Hutchison, Pyle, et al., 2016; McNamara et al., 2018; Rappich et al., 2016). Clearly, these findings bear significant implications for volcanic hazard assessment at Aluto and across the MER, which need to be incorporated into hazard models such as the event tree presented in this work and other possible approaches. Primary volcanic hazards are not the only volcanic hazards: The occurrence of lahars, especially during the rainy seasons, could also be expected at Aluto (e.g., Bekele, 2017), as indicated by numerous volcanoclastic water-sediment-flow deposits found on, and surrounding, the volcanic edifice (e.g., Clarke, 2020; Hutchison, Pyle, et al., 2016). In the following subsection, we provide more details on the current knowledge about eruption sizes and styles at Aluto volcano.

## 2.2. Previous and Contemporary Research at Aluto

The volcanic edifice of Aluto comprises a trachytic shield volcano incised by a  $9 \times 6$  km elliptical caldera (Hutchison, Fusillo, et al., 2016), which has later been buried by the products of numerous pumice cone eruptions, including tephra fall and PDC deposits (e.g., Clarke, 2020; Fontijn et al., 2018; Hutchison, Pyle, et al., 2016). The oldest rocks at Aluto are associated with its trachytic shield stage, comprising  $\sim 570$  ka trachyte lavas and tuffs (Hutchison, Pyle, et al., 2016), partly overlain by lake sediments. Between  $\sim 300$ – $320$  ka, Aluto underwent at least one, and perhaps two, caldera-forming eruptions (Fontijn et al., 2018; Hutchison, Fusillo, et al., 2016; Hutchison, Pyle, et al., 2016), generating low-aspect ratio, peralkaline rhyolite ignimbrites, and leaving a remnant caldera fault scarp in the NE of the caldera (Hutchison, Biggs, et al., 2016; Hutchison, Fusillo, et al., 2016; Hutchison, Pyle, et al., 2016). Since at least 60 ka (Hutchison, Pyle, et al., 2016), volcanism at Aluto appears, based on the geological record, to have been dominated by pumice cone eruptions, which largely buried the underlying geology under proximal fall deposits, relatively widespread tephra fall deposits, small volume ignimbrites, and silicic lava flows (Clarke, 2020; Clarke et al., 2019; Fontijn et al., 2018; McNamara et al., 2018). Due to their ubiquity in the recent eruption record at Aluto, these pumice cone eruptions are considered to be the most representative eruption type for contemporary volcanic hazard assessment (e.g., Clarke et al., 2020). Nevertheless, it is crucial to note that our event tree is wider in purpose and applicability, and it is not exclusively designed to model eruptions similar to pumice cone eruptions (see section 3).

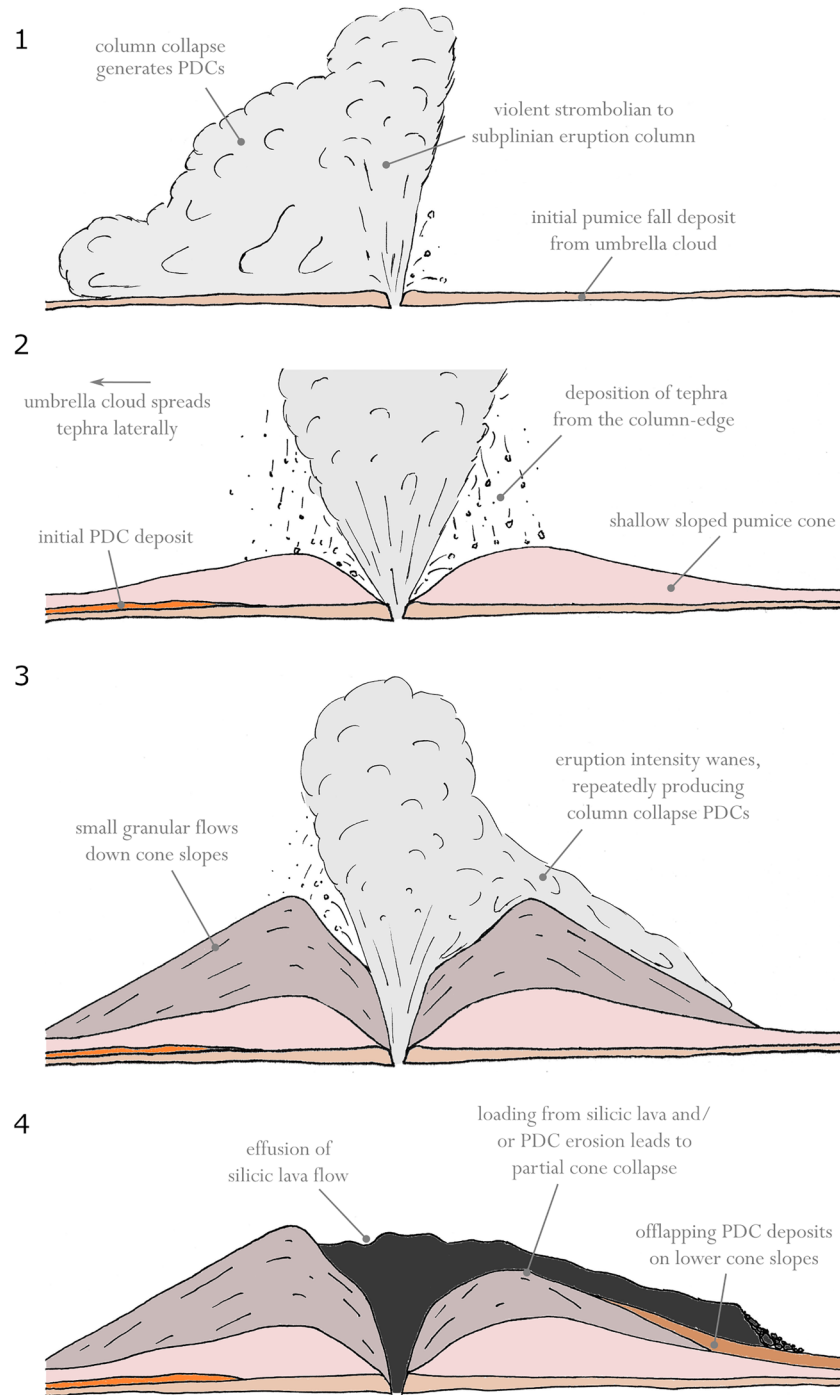


**Figure 2.** A generalized sequence of a pumice-cone building eruption at Aluto volcano, constructed from the geological record of several different, albeit similar, eruptions (modified after Clarke, 2020; Clarke et al., 2020) [Modifications © BGS-UKRI. Modified after © 2020 Clarke et al. Creative Commons Attribution License (CC BY)]. Some pumice-cone forming eruptions began with (1) the generation and collapse of an eruption column, producing tephra fall and PDC deposits. Most eruptions examined at Aluto began with (2) the generation of a convective eruption column, producing relatively widespread tephra fall deposits from the umbrella cloud. Material falling from the edge of the column, and ballistic tephra, built a shallow-sloped pumice cone around the vent. These ultra-proximal deposits built as the eruption progressed to form a steep-sided pumice cone. (3) As the eruption waned, the eruption column became unsteady, repeatedly collapsing and reinitiating, producing intercalated tephra fall and PDC deposits. (4) The eruption ended with the emplacement of a silicic lava flow, which could (or not) have been accompanied by explosive tephra production. The increased load on the pumice cone by the lava flow may result in its partial collapse. Each pumice cone appears to be the product of a single eruption.

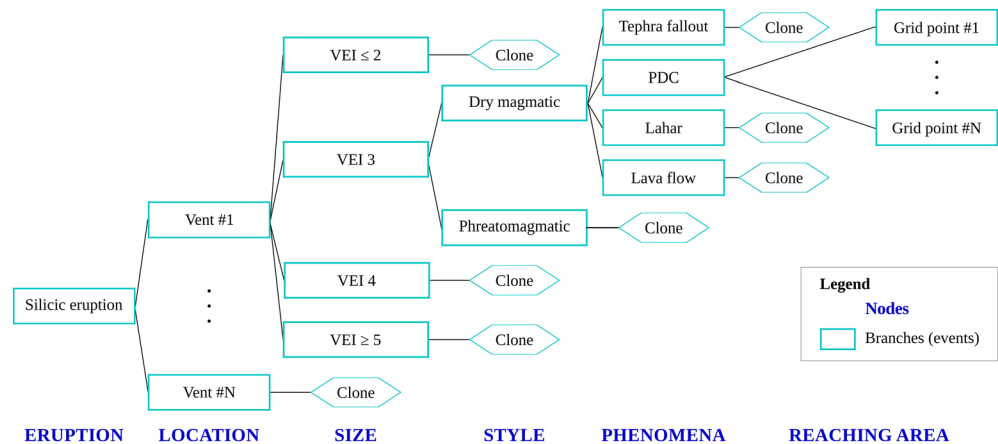


**Figure 3.** Structure of the Aluto event tree presented in this work. “Clone” denotes that the event tree structure is replicated, starting from the node indicated (cf. Newhall & Hoblitt, 2002). Vertical dots in the “location” and “reaching area” nodes indicate the existence of many branches/events. VEI: Volcanic Explosivity Index (maximum event during an eruption), PDC: pyroclastic density current.

Based on geological observations, pumice cone eruptions at Aluto appeared to follow a self-similar eruption sequence (Figure 2), albeit across a range of eruption sizes (Clarke, 2020; Clarke et al., 2019). According to Clarke (2020), most eruptions began with the generation of a pumice cone, thought to be the product of ultra-proximal deposition of pyroclastic material around the vent, with coarse tephra falling from the edge of an increasingly unsteady, convective eruption column, and deposition closer to the vent by ballistic ejection (Clarke et al., 2019; Fontijn et al., 2018). This is effectively the same process as that proposed for “ultra-proximal cones,” which are generated around Plinian eruption vents (Riedel et al., 2003). Toward the top of pumice cone deposits, interbedded fall and PDC deposits are often found, coincident with a decrease in the maximum pumice clast size (Clarke, 2020). This suggests a waning mass eruption rate and an eruption column that repeatedly collapsed (forming PDCs) and re-established (producing tephra fall deposits). This is consistent with the findings of Fontijn et al. (2018) and McNamara et al. (2018), who suggested, largely based on distal terrestrial and lake tephra from Aluto, that pumice cone eruptions were characterized by unsteady eruption columns that may have ranged in intensity from violent Strombolian to sub-Plinian. Pumice cone eruptions at Aluto ended with the emplacement of a silicic lava flow (Clarke, 2020; Fontijn et al., 2018; Hutchison, Pyle, et al., 2016), a feature also recognized at Corbetti, another silicic caldera in the MER (Hunt et al., 2019), and other pumice cones globally (Houghton et al., 1985; Orsi et al., 1989). The explosivity of this final eruption phase is highly uncertain, as the peculiar rheology of peralkaline rhyolite lavas means that it is unclear whether they were emplaced entirely effusively like basaltic lavas or in a syn-effusive-explosive fashion as was observed during recent eruptions of rhyolite lavas at Chaitén (Alfano et al., 2011) and Cordón Caulle (Castro et al., 2013). Work by Hunt et al. (2019) on silicic lava flow morphometry at Corbetti and Fentale volcanoes (other peralkaline rhyolite calderas in the MER) suggests that they closely resemble calc-alkaline rhyolite lava flows and that lava flow emplacement viscosities at Fentale are high, at around  $10^8$ – $10^{11}$  Pa·s. This suggests that rhyolitic, rather than basaltic, lava analogs are most appropriate for this phase of pumice cone eruptions.

### 3. Aluto Event Tree: Using Volcanological Knowledge to Quantify Volcanic Hazard

In Figure 3, we present the event tree model used to conceptualize the Aluto volcanic system and quantify its long-term volcanic hazard. This event tree is the result of a complex iterative process that reflects changes in our understanding of the volcano as well as trade-offs related to the amount and types of volcanological data available for the event tree parameterization (e.g., Marzocchi et al., 2004, 2010; Newhall & Hoblitt, 2002; Newhall & Pallister, 2015). For the interested reader, we report the details of this iterative process, together with previous versions of the Aluto event tree in the supporting information (see Text S1). Below, we focus on describing the structure and parameterization of the Aluto event tree.

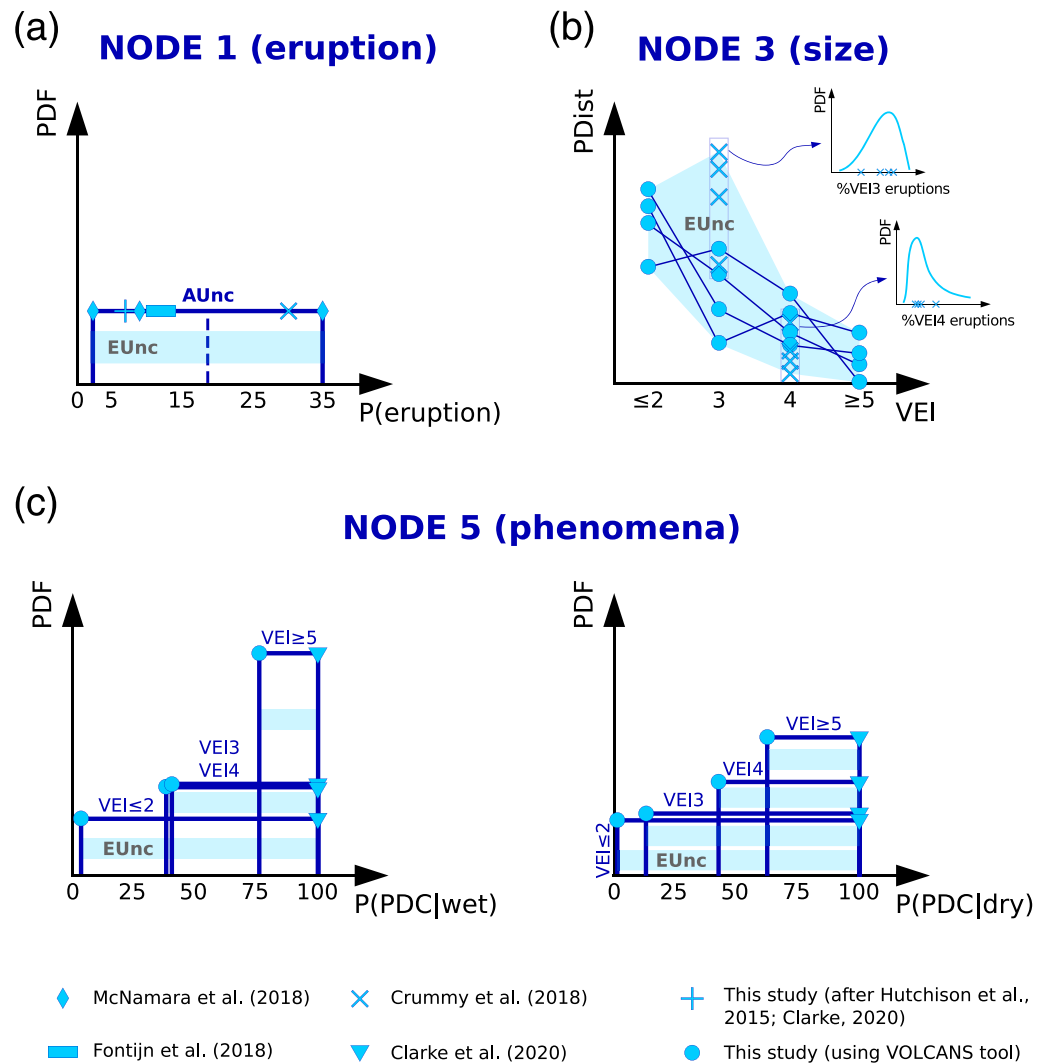


**Figure 4.** Description and evaluation of epistemic uncertainty for Nodes 1 (a), 3 (b) and 5 (c) of the Aluto event tree model. The epistemic uncertainty associated with each node is quantified in a slightly different way, depending on the type and amount of data available and some related assumptions (see sections 3.1, 3.3, and 3.5 for more details). P(-): probability of event; AUnc: aleatory uncertainty; EUnc: epistemic uncertainty; PDF: probability density function; PDist: probability distribution; VEI: Volcanic Explosivity Index; PDC: pyroclastic density current.

The presented event tree is composed of six nodes: eruption, location, size, style, phenomena, and reaching area (Figure 3). Below, we provide the definitions and the reasoning behind the parameterization of each node in the event tree, including estimates for the epistemic uncertainty. We report the specific data sets and probability density functions (PDFs) used to model this epistemic uncertainty in Figure 4 and Tables 1 and 2. The full parameterization of the nodes in the Aluto event tree is provided in Table 3 (e.g., Sandri et al., 2012, 2018). We build a customized version of the event tree model using MATLAB (2012), although we note that there are other tools, such as the BET\_VH (Marzocchi et al., 2010) and PyBET\_VH (Tonini et al., 2015), available for this purpose. A simplified version of an event tree model, which does not account for epistemic uncertainty, is provided in spreadsheet format by Newhall and Pallister (2015).

### 3.1. Node 1: Eruption

1. *Definition:* Long-term occurrence of silicic eruptions at Aluto volcano (including potential initial phreatic phases that evolve into eruptions involving fresh magma). We choose 50 years as the time scale of the analysis, similar to previous volcanic hazard assessments (e.g., Bevilacqua et al., 2016; Sandri et al., 2018).

**Table 1**  
*Different Estimates for the Long-Term Probability of Eruption at Aluto Volcano, According to Diverse Sources of Data Available*

Data source	Return period (year)	Time window	Downscaled eruption rate (eruptions/50 years)	$P(X \geq 1)$	References
Distal pyroclastic deposits (lake cores)	113 <sup>a</sup>	2–12 ka	0.437	35	McNamara et al. (2018)
	519 <sup>b</sup>		0.091	9	
	1700 <sup>b</sup>		0.024	2	
Proximal & distal pyroclastic deposits	250–333	0–12 ka	0.1–0.15	10–14	Fontijn et al. (2018)
Expert elicitation	142	100 kyr	0.352	30	Crummy et al. (2018)
Past eruptive vents	639	0–62 ka	0.077	7	This study (after Clarke, 2020; Hutchison et al., 2015)

*Note.* Average return periods taken from the different sources are converted into average rates of eruptions and used to calculate the probability of at least one eruption in the next 50 years ( $P(X \geq 1)$ ), following a simple Poisson model. Note that each return period is associated with a different time window and that the rates are downscaled to the target time window of 50 years (see section 3.1 for more details). The collection of estimates (expressed in percentage in the table) is interpreted as a representation of the epistemic uncertainty of Node 1 (Eruption) in the event tree (e.g., Marzocchi et al., 2010; Marzocchi & Jordan, 2014; Tierz, Sandri, Costa, Sulpizio, et al., 2016) and modeled using a Uniform PDF that covers the whole range of estimates. In other words, the long-term probability of (at least one) eruption in 50 years is defined as  $P(X \geq 1) \sim \text{Uniform}(2, 35)$  (%).

<sup>a</sup>Average value of “pulses” in McNamara et al. (2018); standard deviation = 13 years. <sup>b</sup>“Quiet periods” in McNamara et al. (2018).

2. *Parameterization:* We make use of four main sources of data to estimate the long-term probability of a silicic eruption. The different estimates reflect the presence of epistemic uncertainty in this node. We model the latter using a Uniform PDF that spans the whole range of estimates, assigning them equal probability (Figure 4a). We sample this PDF ( $10^6$  times) and use these samples to propagate the epistemic uncertainty through the other nodes of the event tree, in a similar way to previous studies (e.g., Sandri et al., 2014, 2018).

The four sources of data are the following: (1) the most recent expert elicitation conducted in April 2018, during the RiftVolc project (Crummy et al., 2018); (2) the tephrochronological study on lake-core tephra layers

**Table 2**  
*Different Estimates for the Probability of Eruption Size, Given Eruption, at Aluto Volcano, According to Diverse Sources of Data Available*

Data source	No. of analogs	$P(\text{VEI} \leq 2)$	$P(\text{VEI} = 3)$	$P(\text{VEI} = 4)$	$P(\text{VEI} \geq 5)$	References
Expert elicitation	—	—	0.305	0.006	—	Crummy et al. (2018)
	—	—	0.714	0.054	—	
	—	—	0.773	0.051	—	
	—	—	0.252	0.102	—	
	—	—	0.564	0.045	—	
	—	—	0.302	0.041	—	
	—	—	0.441	0.033	—	
VOLCANS set 1	50	0.838	0.067	0.095	0.000	This study (after Tierz et al., 2019)
	100	0.747	0.093	0.151	0.009	
VOLCANS set 2	50	0.798	0.017	0.102	0.083	
	100	0.692	0.022	0.199	0.087	
VOLCANS set 3	50	0.738	0.012	0.188	0.063	
	100	0.744	0.021	0.155	0.081	
VOLCANS set 4	50	0.787	0.013	0.133	0.067	
	100	0.766	0.028	0.137	0.069	
Mean		0.764	0.275	0.102	0.057	
Normalized mean		0.637	0.230	0.085	0.048	
Variance		0.002	0.085	0.004	0.001	

*Note.* Each estimate corresponds with a “realization” of the probability distribution for the eruption sizes and the collection of estimates is interpreted as a representation of the epistemic uncertainty of Node 3 (Size) in the event tree (e.g., Marzocchi et al., 2010; Marzocchi & Jordan, 2014; Rougier et al., 2013; Tierz, Sandri, Costa, Sulpizio, et al., 2016). This is modeled using a Dirichlet multivariate PDF whose variable means are equal to the (normalized) mean value of the estimates for each eruption size and whose variance is constrained by the variable with the largest variance ( $P(\text{VEI} = 3)$ ); see section 3.3 for more details and the whole parameterization of the event tree in Table 3). Probabilities are indicated between 0 and 1.

**Table 3**  
Full Parameterization of the Long-Term Event Tree Model for Aluto Volcano, Including Explanation About Whether Epistemic Uncertainty Is Estimated for a Given Node and the Sources of Data Used

Node	Epistemic uncertainty	Sources of data	PDF	Parameters	Values	References
1 (Eruption)	Estimated	Expert elicitation Distal deposits (lake cores) Proximal & Distal deposits Number of eruptive vents	Uni	$p_{1min}$ $p_{1max}$	0.024 0.354	Crummy et al. (2018); McNamara et al. (2018); Fontijn et al. (2018); this study (after Hutchison et al., 2015; Clarke, 2020) After Clarke et al. (2020)
2 (Location)	Not estimated <sup>a</sup>	Location of past vents	Di <sup>b</sup>	$\mu_{2min}$ $\mu_{2max}$	$<1 \cdot 10^{-6}$ 0.006	
3 (Size)	Estimated	Expert elicitation VOLCANOS	Di	$\mu_3$ $\Lambda_3$	[0.637; 0.230; 0.085; 0.048] 5.06	Crummy et al. (2018); this study (after Tierz et al., 2019)
4 (Style)	Very low	weighting schemes A11–4 VOLCANOS	—	$p_4$	“Wet”: [0.05; 0.15; 0.37; 0.43] “Dry”: [0.95; 0.85; 0.63; 0.57]	This study (after Tierz et al., 2019)
5 (Phenomena) <sup>c</sup>	Estimated	weighting schemes A11–4 VOLCANOS	Uni	$p_5$ “Wet” $p_5$ “Dry”	min: [0.03; 0.38; 0.40; 0.77] max: [1.00; 1.00; 1.00; 1.00] min: [0.02; 0.14; 0.43; 0.63] max: [1.00; 1.00; 1.00; 1.00]	This study (after Tierz et al., 2019; Clarke et al., 2020)
6 (Reaching Area) <sup>c</sup>	Not estimated	Proximal deposits + Modeling	—	$p_{6min-max}$	$<0.01-0.12$	Clarke et al. (2020)

Note. PDF: probability density function; Uni: Uniform; Di: Dirichlet;  $p_i$ : probability value in the  $i$ th node;  $\mu_i$ : mean probability of the  $i$ th node;  $\Lambda_i$ : equivalent number of data of the  $i$ th node. Note that for nodes 3, 4, and 5, the values separated by semicolons correspond to eruption sizes: VEI  $\leq 2$ , VEI 3, VEI 4, and VEI  $\geq 5$ , respectively.

<sup>a</sup>Setting the equivalent number of data ( $\Lambda_2$ ) to a very high value would be equivalent to not consider the epistemic uncertainty (e.g., Marzocchi et al., 2008; Sandri et al., 2018). <sup>b</sup>We renormalize the values in Clarke et al. (2020) to ensure that the vent-opening probabilities integrate to 1. <sup>c</sup>We illustrate the parameterization of Nodes 5 and 6 for PDCs only.

by McNamara et al. (2018); (3) the MER-wide stratigraphical study on tephra layers by Fontijn et al. (2018); and (4) a data set of eruptive vents from postcaldera volcanism collected by Hutchison et al. (2015) and refined by Clarke (2020). From all the sources, we extract an average rate of eruptions per time window (the inverse of the average return period, including the current repose time) and use the Poisson distribution to calculate the probability of at least one eruption during the target time window: next 50 years (Table 1).

From Crummy et al. (2018), we take the consensus log-normal PDF for the number of silicic eruptions in any 100 kyr period to calculate the average rate in such time window (~705 eruptions/100 kyr) and downscale it to a 50 year-period average rate (~0.352 eruptions/50 years). Note that this assumes that (1) the number of eruptions per time period at Aluto may follow different distributions depending on the timescale (e.g., log-normal PDF for 100 kyr periods versus Poisson distribution for 50 year periods) and (2) there is not enough evidence against stationarity in the number of eruptions over short time scales (e.g., McNamara et al., 2018, suggested nonstationarity on the scale of several kyr).

From McNamara et al. (2018), given the lack of data spanning the last 2 kyr, we assume that it is not known whether Aluto volcano is currently in a “quiet period” or experiencing a “pulse in activity.” Therefore, we use all the return periods provided by McNamara et al. (2018) to calculate a set of average rates of eruptions, which we downscale to 50 years (Table 1). From Fontijn et al. (2018), we take their average rate of ~2–3 eruptions/kyr and downscale it to 50 years as well.

Finally, based on 96 postcaldera vents (Hutchison et al., 2015; revised by Clarke, 2020), and assuming an age of ~62 ka for the oldest (Hutchison, Pyle, et al., 2016), we estimate at least 0.077 eruptions/50 years (Table 1). We acknowledge that a number of vents, older than those identifiable on the surface, could have been buried by the eruptive products of younger eruptions. Including these “buried vents” would affect the volcanic hazard assessment (e.g., Wetmore et al., 2009). Unfortunately, we lack a data set of buried vents at Aluto. Not being able to consider buried vents has the effect of artificially lowering the estimated average rate of eruptions because we are missing eruptions (i.e., vents). On the other hand, the age of the oldest postcaldera eruptive product remains unclear. Hutchison, Pyle, et al. (2016) dated an obsidian coulée at  $62 \pm 13$  ka. However, Clarke (2020) suggested that this might not correspond to the oldest postcaldera unit, given that it rests on top of a thick pile of postcaldera deposits and has a “relatively fresh-looking topography” (e.g., recognizable ogives, lack of gullying, and a low degree of revegetation) compared to other obsidian lava flows at Aluto (Clarke, 2020). Therefore, if the 96 vents identified had been produced over a period of time longer than ~62 ka, we would be artificially increasing the estimated average rate of eruptions at Aluto volcano. Consequently, the two described effects have opposite implications for our estimate of 0.077 eruptions/50 years.

### 3.2. Node 2: Eruption Location

1. *Definition:* Spatial occurrence of silicic eruptions (i.e., vent opening) at Aluto volcano.
2. *Parameterization:* We apply the same approach as Clarke (2020), based on field evidence that suggests that individual pumice cones are monogenetic and that pumice cone vents are distributed across the edifice (Clarke, 2020; Fontijn et al., 2018; Hutchison, Biggs, et al., 2016; Hutchison, Pyle, et al., 2016). A data set with the locations of 96 past eruptive vents (Clarke, 2020; Hutchison et al., 2015), assumed to have been formed since approximately 55–60 ka (Hutchison, Pyle, et al., 2016), is used to fit a Gaussian symmetric kernel function (e.g., Connor et al., 2018; Connor & Hill, 1995; Weller et al., 2006), with bandwidth ~0.7 km (Clarke et al., 2020), to provide us with a bivariate PDF (UTM Easting-Northing) for the probability of future vent opening at Aluto, given eruption. Given the very limited information about the ages of each of the specific vents, we are not able to reject the hypothesis of temporal stationarity in the vent-opening pattern. In other words, we assume that the data-generating process responsible for the formation of the available data set of vent locations remains meaningful for future vent locations at the volcanic system (e.g., Connor & Hill, 1995). We note that epistemic uncertainty is not quantified at this node, given the scarce information available for this task.

### 3.3. Node 3: Eruption Size

1. *Definition:* Occurrence of silicic eruptions of different VEI sizes at Aluto volcano.
2. *Parameterization:* We use several pieces of evidence to estimate the probability distribution of eruption sizes, given eruption. First of all, we assume that eruption size is independent of vent location. This is

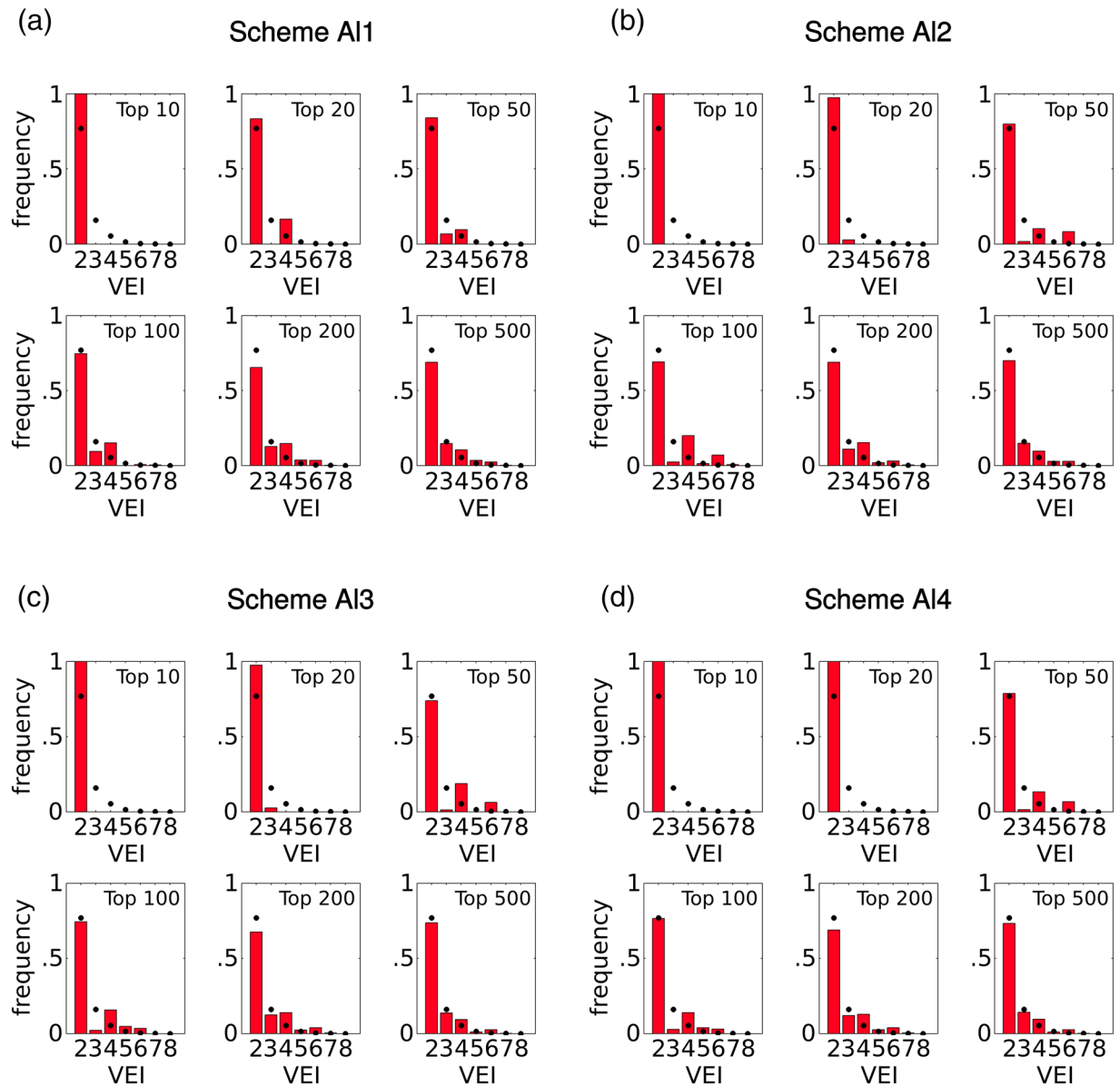


**Figure 5.** Conditional probability distributions of eruption size (VEI) given eruption computed from different sets of analog volcanoes identified using the VOLCANO ANALOGUES SEARCH tool (VOLCANS; Tierz et al., 2019). Four weighting schemes (see below) and different numbers of top analog volcanoes (10, 20, 50, 100, 200, and 500) are explored. Black dots indicate the global probability distribution of VEI given eruption, after correcting for under-recording (Tierz et al., 2019). Please note that “2” on the x-axis denotes “VEI  $\leq$  2.” Weighting schemes used (abbreviations as in section 3.3 and Tierz et al., 2019): A11:  $T_s = 1/3$ ,  $G = 1/3$ ,  $M = 1/3$ ,  $S_z = 0$ ,  $S_t = 0$ ; A12:  $T_s = 0.5$ ,  $G = 0.3$ ,  $M = 0.2$ ,  $S_z = 0$ ,  $S_t = 0$ ; A13:  $T_s = 0.7$ ,  $G = 0.2$ ,  $M = 0.1$ ,  $S_z = 0$ ,  $S_t = 0$ ; A14:  $T_s = 0.9$ ,  $G = 0.075$ ,  $M = 0.025$ ,  $S_z = 0$ ,  $S_t = 0$ .

supported by observations of self-similar eruptive sequences in eruptions of varying sizes and sourced from diverse locations at Aluto volcano (Clarke, 2020; Clarke et al., 2019).

We use data from two different sources to derive probability distributions of eruption size (Figure 4b): (1) the expert elicitation results from Crummy et al. (2018) and (2) sets of top analog volcanoes identified with the VOLCANS tool (Tierz et al., 2019). VOLCANS uses five volcanological criteria (tectonic setting,  $T_s$ ; rock geochemistry,  $G$ ; volcano morphology,  $M$ ; eruption size,  $S_z$ ; and eruption style,  $S_t$ ), and a structured combination of them, to quantify the overall multicriteria volcano analogy between any two volcanoes in the Global Volcanism Program (GVP) database (Global Volcanism Program, 2013). The user is provided with full

flexibility in the choice of the weights assigned to each criterion, when calculating the multicriteria analogy (which represents a weighted average of single-criterion analogy values, Tierz et al., 2019).

We take the probability distribution of eruption sizes for each top analog volcano, sample it randomly  $10^4$  times, cumulate the samples for each eruption size, and recompute a merged probability distribution of eruption sizes, by combining the samples from all top analog volcanoes. We test the influence of the number of top analog volcanoes used (10, 20, 50, 100, 200, and 500) in the estimates obtained for the merged probability distributions (Figure 5). We note that if the number of analog volcanoes is small (e.g., 10 and 20), the computed probability distribution can be very unstable and not necessarily realistic (Figure 5). If the number of analog volcanoes used is too high (e.g., 500), the probability distributions start to approximate the global probability distribution of eruption sizes (e.g., Papale, 2018; Rougier et al., 2018), because we are using almost one in every three volcanoes in the database. We find that using an intermediate number of analog volcanoes can be a good compromise between deriving a probability distribution of VEI sizes that may be characteristic of the volcano of interest and obtaining realistic, stable estimates of the probability of different eruption sizes. In this work, we use 50 and 100 top analog volcanoes (see Data Sets S1–S4) to derive the probability distributions of VEI sizes to parameterize our event tree model.

We explore four different weighting schemes in VOLCANS, all of which give preference (i.e., higher weights) to tectonic setting over rock geochemistry over volcano morphology (NB). (We remove the rock type “Dacite” from the GVP profile of Aluto volcano to run VOLCANS, because there is no evidence to support the presence of such rock type in the post-caldera erupted products of Aluto, e.g., Clarke et al., 2019; Fontijn et al., 2018; Hutchison, Pyle, et al., 2016; Hutchison et al., 2018; Iddon et al., 2019; McNamara et al., 2018). The reasoning behind this choice is that peralkaline volcanic systems are more likely to be tied to tectonic settings similar to that of Aluto, especially because the GVP database, and thus VOLCANS, do not differentiate peralkaline and metaluminous rock suites (Siebert et al., 2010). Volcano morphology is given the lowest weight in all the explored weighting schemes because the intermediate value that Aluto has for the simplified morphology metric used by VOLCANS ( $M_{Aluto} = 0.579$ ) is quite similar to the mean value of shield volcanoes (mean ( $M_{shields}$ ) = 0.567, Tierz et al., 2019). Therefore, giving a high weight to the volcano morphology criterion might generate some misleading sets of analog volcanoes (e.g., dominated by basaltic shield volcanoes).

We obtain eight different estimates for the distribution of probability of eruption size, given eruption, from VOLCANS (Table 2). From the expert elicitation of Crummy et al. (2018), we take another eight estimates for the probability of VEI 3 and VEI 4 eruptions, by randomly sampling the PDFs of the variable “number of VEI 3 and VEI 4 eruptions per 10,000 eruptions at Aluto volcano” (Crummy et al., 2018). The probability of smaller and bigger eruptions was not assessed in this expert elicitation. The different probability distributions derived for the eruption size at Aluto volcano inform us of the presence of epistemic uncertainty for the probability of different eruption sizes. We model this uncertainty using a Dirichlet multivariate PDF (e.g., Marzocchi et al., 2008, 2010), which assumes that the eruption sizes defined are mutually exclusive and exhaustive events. We parameterize the Dirichlet PDF by calculating the mean of each of the variables (i.e., VEI sizes) as equal, respectively, to the normalized mean probability for each eruption size, as computed from the different available sources (Table 2), and using the largest variance—P (VEI 3), Table 2—to calculate the “number of equivalent data,”  $\Lambda$ , for the Dirichlet PDF (see equations 6 to 11 in the supplementary material of Marzocchi et al., 2008). The latter represents a way of expressing the variance of the distribution and can be understood, under a Bayesian perspective, as the number of (past) data required to significantly modify the posterior distribution, by Bayesian updating, from the prior distribution (e.g., Marzocchi et al., 2008, 2010). Like in Node 1, we sample the target PDF ( $10^6$  times) and use these samples to propagate the epistemic uncertainty through the other nodes of the event tree (e.g., Sandri et al., 2012, 2014, 2018).

### 3.4. Node 4: Eruption Style

1. *Definition:* Occurrence of different eruptive styles (dry magmatic and phreatomagmatic) during silicic eruptions at Aluto volcano.
2. *Parameterization:* We rely on data coming from the GVP 4.6.7 database (Global Volcanism Program, 2013) to estimate the proportion of eruptions, for each eruption size, that may display phreatomagmatic or dry volcanic activity only. We note that, although there is constant updating and upgrading of the GVP resources, some inadequacies may still be present in the data set (e.g., Ogburn et al., 2015;

Siebert et al., 2010; Tierz et al., 2019). We treat these two events as mutually exclusive and exhaustive events, that is, each eruption may include phreatomagmatic activity or not.

In Node 3, data coming from sets of top analog volcanoes were used to calculate the probability distributions of eruption size. In Nodes 4 and 5, we use data from any volcanic system in the GVP database that has eruptions with phreatomagmatic activity. We then weight the data coming from each different volcano according to its degree of analogy calculated with VOLCANS (see Data Set S5). This allows us to compute the probability of phreatomagmatic and dry magmatic eruptions at Aluto volcano and accounting for the degree of analogy between each available volcano and our target volcano (Tierz et al., 2019). The formula used is the following:

$$f_{ph}(x) = \frac{\sum_i^I \sum_j^J 1_{ij}(x) A_{iAluto}}{\sum_i^I \sum_j^J A_{iAluto}} \quad (1)$$

where  $f_{ph}(x)$  is the frequency of phreatomagmatic eruptions for VEI size  $x$ ,  $1_{ij}(x)$  is the indicator function for the  $j$ th eruption of size  $x$  at volcano  $i$ , and  $A_{iAluto}$  is the multicriteria analogy value between volcano  $i$  and Aluto volcano. In this way, the presence or absence of phreatomagmatic eruptions from volcanoes with high value of analogy with Aluto will count more in the final calculation of  $f_{ph}(x)$ . If all volcanoes in the available data set had the same value of multicriteria analogy with Aluto, formula (1) would return the *classical* frequency, that is, total number of phreatomagmatic eruptions divided by the total number of eruptions.

We use the same four weighting schemes as in Node 3 to calculate the multicriteria analogy between the available set of volcanoes and Aluto, using VOLCANS. The different estimates obtained for the conditional probability of dry magmatic and phreatomagmatic eruptions at Aluto are a representation of the epistemic uncertainty for this node. We note that these estimates differ by a maximum value of  $8 \cdot 10^{-3}$ , across all eruption sizes. Given these very low values, we choose not to model the epistemic uncertainty in this node (see Table 3).

### 3.5. Node 5: Hazardous Phenomena

1. *Definition:* Generation of different hazardous phenomena (tephra fallout, PDCs, lahars, and lava flows) during and/or after in the case of lahars, silicic eruptions at Aluto volcano.
2. *Parameterization:* We also use the GVP 4.6.7 database to extract data on the occurrence of different volcanic hazardous phenomena. We use the same set of volcanoes as in Node 4 and weight their data according to the analogy values computed from VOLCANS, using the same weighting schemes as in Nodes 3 and 4. The probability of generation of each hazardous phenomenon is conditioned upon both the eruptive style (i.e., dry magmatic and phreatomagmatic eruptions) and the eruption size (VEI), the latter being particularly important for phenomena such as PDCs (e.g., Newhall & Hoblitt, 2002; Sandri et al., 2018). Also, in the same way as in Node 4, we use four different weighting schemes to calculate the multicriteria analogy between the available set of volcanoes and Aluto, using VOLCANS. This provides us with a representation of epistemic uncertainty for Node 5 (Uniform PDFs covering the range of conditional probabilities, Figures 4c–4d) which we explore by sampling the Uniform PDF and propagate through the other nodes of the event tree. In the case of PDCs, we extend the upper limit of the Uniform PDF to 1, to include a somewhat “maximum hazard,” precautionary estimate as in Clarke et al. (2020). In other words, any value of the probability of PDC occurrence given eruption below 1 would represent a lower PDC hazard. Note that our estimations of the probability in nodes 4 and 5 are not specifically designed for caldera-forming eruptions, although the latter are included in relation to the  $VEI \geq 5$  branch/event.

### 3.6. Node 6: Reaching Area of Hazardous Phenomena

1. *Definition:* Occurrence of different hazardous phenomena on specific points around the volcano.
2. *Parameterization:* We refer to Clarke et al. (2020) for an example of a probabilistic hazard assessment of PDC invasion at Aluto, conditional on the occurrence of a silicic eruption producing PDCs at the volcano. In that work, the authors used an Energy Cone-Monte Carlo approach (e.g., Sandri et al., 2018; Tierz et al., 2016; Tierz, Sandri, Costa, Sulpizio, et al., 2016) to quantify aleatory uncertainty in PDC

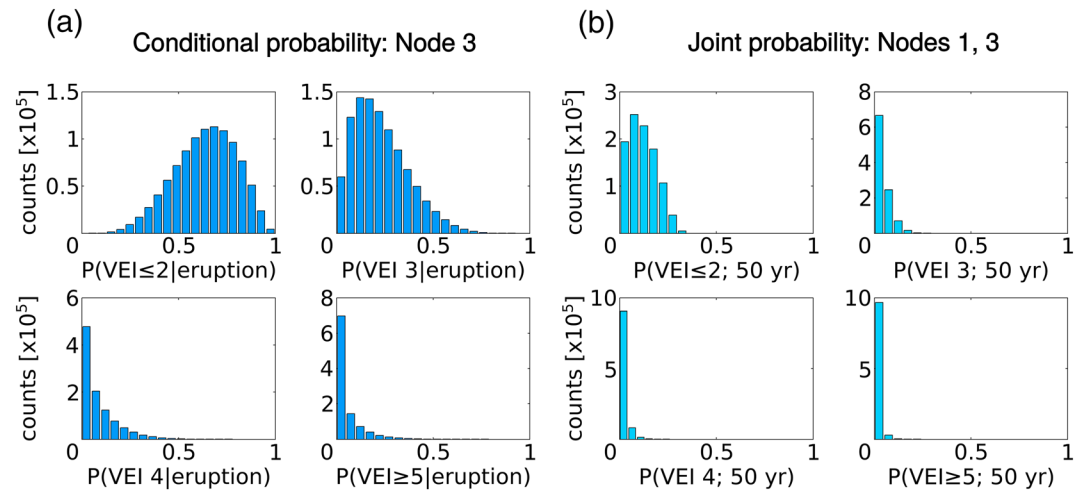


**Figure 6.** Conditional and joint probabilities of eruption size at Aluto volcano, as computed with the event tree model presented in this work. (a) Conditional probability of eruption size (VEI) given eruption at Aluto, accounting for epistemic uncertainty; (b) Joint probability of eruption (in 50 years) and eruption size (VEI) at Aluto, accounting for epistemic uncertainty. Node numbering as in Figure 3.

inundation at Aluto. They built PDFs for the collapse height ( $H_0$ ) and effective friction ( $\phi$ ) parameters of the energy cone that were applicable across the expected eruption intensities for pumice cone eruptions at Aluto (Clarke et al., 2020), without an explicit partition in terms of VEI. The PDF for  $H_0$  was derived from an innovative multimodel strategy that uses the PlumeRise model of Woodhouse et al. (2013) to constrain the height of the top of the gas-thrust region for eruptive conditions expected at Aluto (Clarke et al., 2020; Ben Clarke, unpublished data). The PDF for  $\phi$  was obtained from pumice-flow data in Ogburn (2012), after manually filtering the data set for PDCs that resembled those interpreted from the deposits studied at Aluto volcano (Clarke, 2020; Clarke et al., 2020). PDC volumes of the selected pumice flows ranged between approximately  $10^4$  and  $10^8$  m<sup>3</sup>. The development of other parameterizations for alternative hazardous phenomena is discussed in section 5.1.

#### 4. Event Tree Results

We illustrate a few examples of joint, marginal, and conditional probabilities for different volcanic events that can be derived through the event tree model. These can be loosely interpreted as *eruption scenarios* or *eruptive settings* (e.g., Biass et al., 2016; Marzocchi et al., 2010; Sandri et al., 2014; Selva et al., 2010; Tierz et al., 2018). It is important to note that event tree models, like other volcanic hazard models, are quantitative tools that offer the user full flexibility on the choice of scenarios to be explored. The focus on specific scenarios is seldom based on volcanological grounds exclusively (Papale, 2017), due to the complicated links between volcanic hazard and risk management under uncertainty at volcanic systems (e.g., Aspinall et al., 2002; Marzocchi et al., 2012; Marzocchi & Woo, 2007).

##### 4.1. Occurrence of Silicic Eruptions

Considering all available estimates, the long-term (50 years) probability of one or more silicic eruptions at Aluto volcano ranges from 2% to 35% (Table 1), both estimates are from assumptions based on McNamara et al. (2018). The estimate based on the number of postcaldera past vents identified at the surface is closer to the lower limit while the estimate based on the elicitation exercise by Crummy et al. (2018) is closer to the upper limit. The estimates from the work of Fontijn et al. (2018) are closer to the mean of the Uniform distribution (Figure 4a). The effect of the epistemic uncertainty on the long-term probability of silicic eruptions at Aluto is reflected in the estimates of the probability of eruption size and occurrence of PDCs (see next subsections).

##### 4.2. Size of Silicic Eruptions

We report the values for conditional (i.e., eruption size given silicic eruption, Figure 6a) and joint (i.e., silicic eruption and eruption size, Figure 6b) probabilities for the size of silicic eruptions at Aluto, including the

effect of epistemic uncertainty on both nodes 1 and 3 of the event tree. The mean conditional probability of  $VEI \leq 2$  is around 67%, making it the most-likely eruption size in future eruptions, followed by VEI 3 eruptions, with a mean conditional probability of 23%. The mean conditional probability for  $VEI \geq 5$  eruptions at Aluto is just below 5% (Table 2). Although the parameterization of our event tree does not consider  $VEI \geq 6$  eruptions separately, we report here that the mean conditional probability of occurrence of VEI 6 and VEI 7 eruptions, respectively, is about 4% and 0.1%, considering the eight different sets of analog volcanoes from VOLCANS used to parameterize the event tree (see Figure 5, Table 2, and Data Sets S1–S5).

The effect of epistemic uncertainty on the conditional probability for  $VEI \leq 2$  and VEI 3 eruptions is significant (Figure 6a). In the case of VEI 4 and  $VEI \geq 5$  eruptions, their marginal Beta PDFs indicate that they are unlikely to occur but, accounting for epistemic uncertainty, their maximum conditional probabilities of occurrence can be above 80%. It should be noted that any sample from the variables of the Dirichlet PDF (i.e., conditional probability of eruption sizes) sums up to 1; therefore, if the conditional probability of, for example, a VEI 4 eruption is high, for that sample, the conditional probabilities for the remaining VEI sizes must be lower in order to satisfy this requirement.

In terms of the joint probability of eruption and eruption size (Figure 6b),  $VEI \leq 2$  and VEI 3 eruptions are the most likely but, when we consider the long-term probability of eruption and its epistemic uncertainty, the probability values are much lower and their marginal distributions are all positively skewed and, more skewed in general. This implies that the probability of eruptions of different sizes in the next 50 years are generally low. For example, the mean probability of  $VEI \leq 2$  is 12%, and mean probabilities for VEI 3 or VEI 4 eruptions are about 4% and 2%, respectively. However, it is also observed that, considering the epistemic uncertainty, there is a nonzero likelihood that the (true) probability of  $VEI \geq 5$  eruptions in the next 50 years may be almost 25% (Figure 6b).

### 4.3. Occurrence of Pyroclastic Density Currents

We explore the probability of occurrence of one of the most hazardous volcanic phenomena: PDCs. We focus on the marginal probability of PDCs in the next 50 years,  $P(\text{PDC}; 50 \text{ years})$ , and explore the PDFs obtained when taking into account the epistemic uncertainty in different nodes of the event tree model for Aluto volcano. To obtain this marginal probability, we use the following formula:

$$\begin{aligned}
 P(\text{PDC}; 50 \text{ years}) &= \\
 \sum_i \sum_j P(\text{eruption}_{50 \text{ years}}, \text{ersize}_i, \text{erstyle}_j, \text{PDC}) &= \\
 P(\text{PDC} | \text{eruption}_{50 \text{ years}}, \text{ersize}_i, \text{erstyle}_j) P(\text{style}_j | \text{eruption}_{50 \text{ years}}, \text{ersize}_i) \dots & \quad (2) \\
 P(\text{ersize}_i | \text{eruption}_{50 \text{ years}}) P(\text{eruption}_{50 \text{ years}}) &= P(\text{PDC} | \text{ersize}_i, \text{erstyle}_j) P(\text{erstyle}_j | \text{ersize}_i) \\
 P(\text{ersize}_i | \text{eruption}_{50 \text{ years}}) P(\text{eruption}_{50 \text{ years}}) &
 \end{aligned}$$

where  $\text{eruption}_{50 \text{ years}}$  is the long-term probability of silicic eruption,  $\text{ersize}_i$  is the probability of the  $i$ th eruption size,  $\text{erstyle}_j$  is the probability of the  $j$ th eruption style (i.e., wet or dry eruptions). Note how the independencies borne by the event tree model (e.g.,  $P(\text{erstyle}_j \perp \text{eruption}_{50 \text{ years}} | \text{ersize}_i)$ ) permit simplification of some terms in Equation 2.

In particular, we compute the following cases for  $P(\text{PDC}; 50 \text{ years})$ : (1) only epistemic uncertainty for Node 5 (Figure 4c) is incorporated, while the mean probabilities (i.e., aleatory uncertainty only) are used in Nodes 1 and 3 (Figure 7a); (2) only epistemic uncertainty for Node 1 (Figure 4a) is incorporated, while the mean probability for Node 3 and the maximum probability for Node 5 (Clarke et al., 2020) are used (Figure 7b); (3) epistemic uncertainty for Nodes 3 and 5 (Figures 4b and 4c) is incorporated, while the mean probability for Node 1 is used (Figure 7c); and (4) all the epistemic uncertainty accounted for in our event tree model is incorporated (Figure 7d).

Several aspects are evidenced in these graphs. First of all, not only the extent of the epistemic uncertainty for  $P(\text{PDC}; 50 \text{ years})$  changes between graphs but, importantly, also the shape of the PDF is modified. The latter, in turn, conditions the estimate for the aleatory uncertainty as the mean of the distribution (dashed line

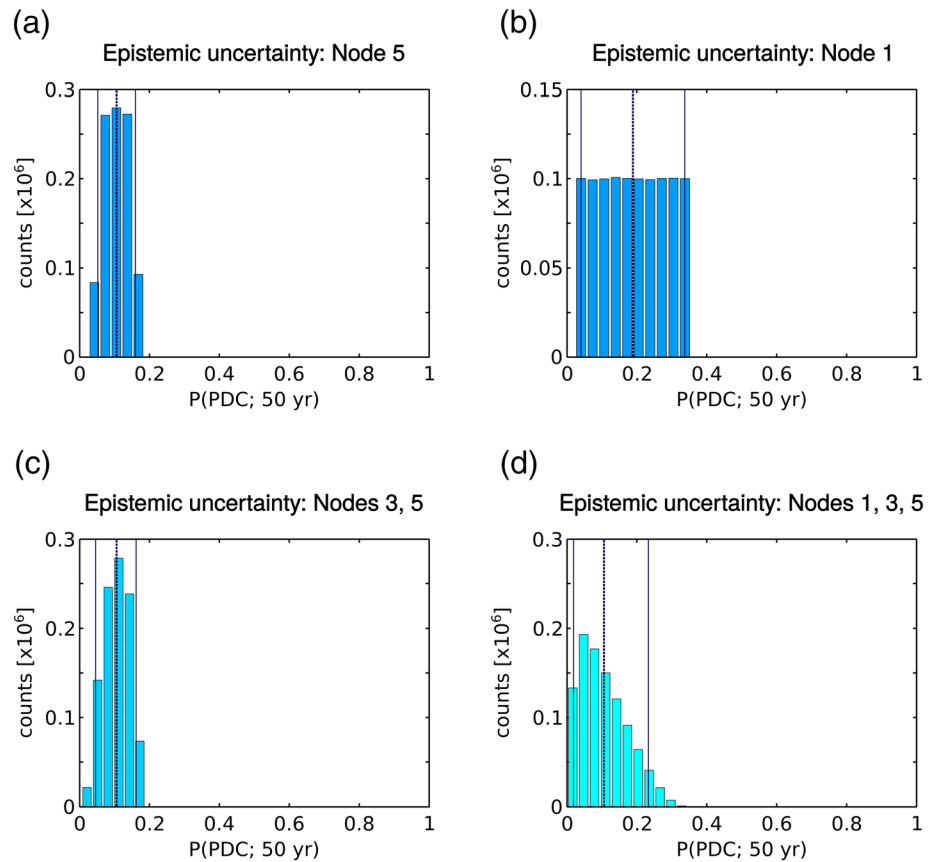


**Figure 7.** Marginal probability of PDC occurrence in 50 years (see formula 2) at Aluto volcano, as computed with the event tree model presented in this work. Different insets illustrate the effect on this marginal probability of incorporating the epistemic uncertainty of different nodes within the event tree: (a) epistemic uncertainty in the conditional probability of PDC occurrence, given eruption size and eruption style (Node 5); (b) epistemic uncertainty in the probability of eruption in 50 years (Node 1); (c) epistemic uncertainty in the conditional probability of eruption size given eruption and in the conditional probability of PDC occurrence, given eruption size and eruption style (Nodes 3 and 5); (d) epistemic uncertainty in the probability of eruption in 50 years, in the conditional probability of eruption size given eruption and in the conditional probability of PDC occurrence, given eruption size and eruption style (Nodes 1, 3, and 5). Solid lines denote the mean of the distribution sample and dashed lines denote the 5th and 95th percentiles (90% credible interval) of the distribution sample.

in Figure 7). The extent of the epistemic uncertainty can be expressed, for instance, as the interval between lower and upper percentiles of the PDF for  $P(\text{PDC}; 50 \text{ years})$ . We use the 5th and 95th percentiles (solid lines in Figure 7) to stress the effect of skewed PDFs in the interval (Figure 7d). According to our estimates, the extent of the epistemic uncertainty is largest when considering the epistemic uncertainty in  $P(\text{eruption}_{50 \text{ years}})$  only (about 30%, between 4% and 34%, Figure 7b) and smallest when considering the epistemic uncertainty in  $P(\text{PDC}|\text{er}_{size_i}, \text{er}_{style_j})$  only (around 11%, between 5% and 16%, Figure 7a). When accounting for the epistemic uncertainty in Nodes 1, 3, and 5, the extent of the total epistemic uncertainty for  $P(\text{PDC}; 50 \text{ years})$  is approximately 21%, between 2% and 23% (Figure 7d). This may seem counter-intuitive because one may think that the more epistemic uncertainty is accounted for, the greater the overall extent of the epistemic uncertainty in the final computed PDF. However, this extent depends on (a) the specific node where the extent of epistemic uncertainty is being evaluated (Node 5 in our case); (b) the node(s) where the epistemic uncertainty is being accounted for (different combinations of Nodes 1, 3, and 5, in Figure 7); and, finally, (c) the combinatorial probabilistic calculations that take place to compute the final PDF, which depend on the location and shape of the different PDFs involved (e.g., the multiplication of samples drawn from two Uniform distributions tends to an exponential-like distribution).

In our explored examples, the epistemic uncertainty in Node 1 (eruption) is of paramount importance because its aleatory and epistemic uncertainties propagate into the calculation of the probability of any of the nodes in the model. In Figure 7b, given that we assume  $P(\text{PDC|eruption}) = 1$  (see above), we are actually displaying the long-term probability of eruption. In other words, if  $P(\text{PDC|eruption}) = 1$ , then  $P(\text{PDC}; 50 \text{ years}) = P(\text{eruption}; 50 \text{ years})$ . The estimates of  $P(\text{PDC}; 50 \text{ years})$  when considering the epistemic uncertainty in Nodes 3 (size) or Nodes 3 and 5 (phenomena) are relatively similar (Figures 7a and 7c). In the latter case, both the mean probability and the minimum probabilities are slightly lower, likely due to the incorporation of estimates for  $P(\text{VEI} \leq 2)$  and  $P(\text{VEI} = 3)$  that are above the mean (Figure 6a) and because these small eruption sizes tend to have conditional probabilities of PDC occurrence that are lower than those of larger eruption sizes (Figure 4c). Finally, when the epistemic uncertainty in all the nodes is accounted for, the overall effect is that of making the PDF for  $P(\text{PDC}; 50 \text{ years})$  more skewed (Figure 7d). When compared to Figure 7c, the incorporation of the epistemic uncertainty in  $P(\text{eruption}; 50 \text{ years})$  results in low values of  $P(\text{PDC}; 50 \text{ years})$  being more likely, due to the incorporation of below-average estimates of the former probability. However, it also results in high values of  $P(\text{PDC}; 50 \text{ years})$  being more likely, due to the incorporation of above-average estimates. In other words, the PDF displayed in Figure 7d has collapsed and spread around the mean probability, compared to the PDF in Figure 7c, and this has the effect of increasing the overall extent of the epistemic uncertainty from 12% in the latter to 21% in the former.

## 5. Discussion

### 5.1. Probabilistic Volcanic Hazard Assessment at Aluto

The event tree model presented here represents a framework to quantify volcanic hazard at Aluto volcano that can be coupled with hazard assessments for specific hazardous phenomena to compute integrated PVHA, similar to other volcanic systems (e.g., Bartolini et al., 2014; Becerril et al., 2014; Sandri et al., 2014, 2018; Tierz et al., 2018). The development of the event tree at Aluto benefits from the availability of indispensable volcanological data derived from past and recent research activities (Clarke, 2020; Clarke et al., 2019; Dakin & Gibson, 1971; Di Paola, 1972; Fontijn et al., 2018; Hutchison, Fusillo, et al., 2016; Hutchison, Pyle, et al., 2016; Kebede et al., 1985; McNamara et al., 2018). The parameterization of the event tree is an attempt to incorporate diverse sources of information, as aleatory and, especially, epistemic uncertainty, that can be relevant in terms of the overall volcanic hazard that the volcano poses. Unfortunately, there still remain substantial gaps in our knowledge of the eruptions at Aluto (e.g., eruption ages, volumes, mass eruption rates, spatial distribution of PDC and other types of deposits, etc.), so epistemic uncertainty remains a key element of the PVHA. In particular, the epistemic uncertainty in the long-term probability of eruption has a fundamental role for the event tree assessments (Figures 6 and 7). One possible strategy to reduce this epistemic uncertainty is through additional fieldwork and dating of volcanic products in the proximal and medial sectors of the volcano. For instance, this may help unravel whether Aluto volcano is currently on a “quiet” period or a “pulse” (McNamara et al., 2018) or even if such nonstationary behavior is expected to hold on the timescale of the last 2–3 kyr. Concerning eruption size, there is very little information for Aluto, apart from a  $\sim\text{VEI} 3\text{--}4$  event (Fontijn et al., 2018; Hutchison, Pyle, et al., 2016). Further fieldwork would be required to map deposits and derive a collection of erupted volumes for eruptions at Aluto. This would serve to better understand what the aleatory uncertainty (i.e., the true distribution of eruption sizes) may be at the volcano. Additional expert elicitations (e.g., Crummy et al., 2018; Jenkins et al., 2015) can also help reduce the epistemic uncertainty, as it has been demonstrated elsewhere how repeating this type of exercises can foster consensus among the group of experts (e.g., Selva, Marzocchi, et al., 2012). Our approach of using VOLCANS stands as an innovative avenue to try to tackle the problem of data scarcity. The results obtained using this tool seem reasonable, considering the current state of knowledge about Aluto volcano. As previously introduced, these results include the (unlikely) possibility of very-large-size eruptions (e.g.,  $\text{VEI} \geq 6$ ) at the system. Nevertheless, it must be noted that one current problem with this approach is that the analogs identified for rift volcanoes may tend to be data-scarce themselves (e.g., very few to no eruptions stored in the global databases). Consequently, there is an urgent need to incorporate recent volcanological knowledge on rift volcanism (e.g., Clarke, 2020; Clarke et al., 2019; Fontijn et al., 2010, 2012, 2018; Hunt et al., 2019, 2020; Hutchison et al., 2018; Hutchison, Biggs, et al., 2016; Hutchison, Fusillo, et al., 2016; Hutchison, Pyle, et al., 2016; Martin-Jones et al., 2017; McNamara et al., 2018; Rappich et al., 2016; Sieburg et

al., 2018; Vye-Brown et al., 2016; Wadge et al., 2016) into relevant databases that can be used to compute PVHA (Tierz, 2020).

## 5.2. Portability of Event Trees Across the Main Ethiopian Rift

Event tree models are very useful hazard tools that have been widely applied to a large number of volcanic systems worldwide (see, for instance, Newhall & Pallister, 2015). Three main advantages make them particularly suitable to quantify volcanic hazard at different volcanoes. Firstly, their design and structure are generic (Marzocchi et al., 2008, 2010; Newhall & Hoblitt, 2002), meaning that event trees can be easily adapted to a particular volcano (e.g., Aspinall et al., 2002; Newhall & Pallister, 2015; Queiroz et al., 2008; Sobradelo & Martí, 2010). Secondly, once implemented, the structure of the event tree for a particular volcanic system tends to be stable in time, particularly during noneruptive periods. That is, changes in the event tree parameterization may occur in time as new information becomes available, but the structure may remain virtually the same (e.g., Somma-Vesuvius, Italy; Marzocchi et al., 2004, 2008; Sandri et al., 2009, 2016, 2018; Tierz et al., 2017, 2018). Finally, event trees are easy to understand, visualize, and model because of the partitioning of volcanic events in nodes and branches. This modularity is beneficial both conceptually (i.e., different structures can be explored and discussed, see Text S1 and Figure S1) and computationally (i.e., nonconsecutive nodes tend to be independent of each other, given the intermediate node; therefore, the calculation of conditional and joint probabilities is simplified, e.g., Newhall & Hoblitt, 2002; Marzocchi et al., 2008, 2010; Sobradelo & Martí, 2010). However, event trees also have some notable limitations such as (a) they are not optimal for dynamic hazard modeling, in the context of short-term variations in the probability of occurrence of hazardous phenomena related to changes in triggering factors or mechanisms (e.g., Tierz et al., 2017; Wolpert et al., 2018); and (b) they are not the best suited model for “intra-eruption forecasting,” that is, modeling transitions between eruptive styles during a given eruption, especially when the types of eruptive phases/stages are numerous and/or their temporal sequences are long and complex (e.g., Bebbington & Jenkins, 2019; Cassidy et al., 2018; Jenkins et al., 2007; Ogburn et al., 2015; Sheldrake et al., 2016). We acknowledge that event trees have been previously applied to intraeruption forecasting (e.g., Aspinall et al., 2002; Monserrat Volcano Observatory et al., 1998; Newhall & Pallister, 2015; Wright et al., 2019) but suggest that other statistical models, such as Markov Chain models (e.g., Aspinall et al., 2006; Bebbington, 2007; Bebbington & Jenkins, 2019), may be better suited for this purpose. In any case, we also remark that defining “intraeruption” is implicitly associated with defining “eruption,” which still remains a very complicated issue in modern volcanology (e.g., Bebbington & Jenkins, 2019; Sheldrake et al., 2016; Siebert et al., 2010; Wadge et al., 2014). Finally, it is important to note that event trees can be combined with other uncertainty quantification techniques (e.g., Sandri et al., 2018; Tierz et al., 2017, 2018), and this could potentially help alleviate the aforementioned issues.

Notwithstanding the described limitations, we suggest that event trees could be a key tool to quantify volcanic hazard at silicic centers and basaltic volcanic fields across the MER and, generally, East Africa. The parameterization, and probably the structure, of event trees for different volcanoes in the region will need to be different than the one presented here for Aluto, for instance, to reflect differences in eruptive activity at each volcanic system (e.g., phreatomagmatic activity and hazardous phenomena). Some volcanoes may show a tendency to source eruptions that are either predominantly explosive or effusive from different areas. For example, at Corbetti caldera, based on geological studies, the Urji edifice, on the central-western caldera floor, has mostly erupted explosively while the Chabbi edifice, on the eastern rim of the Corbetti caldera, has mostly erupted obsidian lava flows (Fontijn et al., 2018; Martin-Jones et al., 2017; Rappich et al., 2016). These particularities must be reflected in the event tree models that aim to quantify volcanic hazard at each volcanic system. It is of course also important to recognize that there are uncertainties in the geological record in terms of exposure and preservation of the deposits of past eruptions (e.g., Engwell et al., 2013).

The opportunity to parameterize different event trees using analog volcanoes as a proxy for the volcano of interest has been preliminarily shown here for Aluto using the newly developed VOLCANS tool (Tierz et al., 2019). This allows us to fully parameterize the event tree, including estimates of epistemic uncertainty. A finer-tuned search for analog volcanoes could also be explored, which could start from (subjectively) removing some analogs from the sets identified with VOLCANS. Some good analogs for Aluto that have been previously proposed are the following: Pantelleria, Italy (Clarke, 2020; Crummy et al., 2018; Fontijn et al., 2018; Jenkins et al., 2015); Monte Pilato, Lipari, Italy (Crummy et al., 2018; Fontijn et al., 2018),

Newberry, USA (Crummy et al., 2018), Tuhua/Mayor Island, NZ (Clarke, 2020; Jenkins et al., 2015), Gran Canaria, Spain (Jenkins et al., 2015), and peralkaline caldera systems in general (Clarke, 2020; Mahood, 1984). It should be noted that, given the acute data scarcity across the MER, fine-tuning the analog search may be challenging and the derived sets of analog volcanoes may have very few volcanoes to use. In the end, to estimate a given hazard variable of interest (e.g., distribution of VEI sizes), it might remain a compromise between choosing a *one-for-all* parameterization (e.g., Mastin et al., 2009), using one or very few analog volcanoes; or an *all-for-one* parameterization (Tierz et al., 2019), where more general analogs are identified and a larger set of them is used to obtain an average estimate of the hazard variable. Better understanding and optimizing this trade-off between the amount of objectivity and subjectivity that is introduced in a given set of analog volcanoes will likely be a topic for future research.

### 5.3. Challenges of Building Event Trees at Rift Volcanoes

Despite the potential of event tree models to be adapted to different volcanoes across the MER, it is also important to note some general and setting-specific challenges implied in building an event tree for a peralkaline caldera in a continental rift.

#### 5.3.1. Bimodal Magmatism

The occurrence of bimodal magmatism complicates the design of the “Eruption” and “Location” nodes (Figure S1). In any bimodal volcanic system, the hazard analysis should acknowledge the possibility of different magma compositions being erupted across a given (large) area. One major challenge is understanding the coupling between the feeding systems of the two end-member geochemical compositions. For example, in Iceland, the geochemical evidence suggests that central volcanoes are more likely to erupt evolved magma compositions, but fissure swarms, which typically erupt basaltic magmas, belong to the same feeding system as the evolved magmas (e.g., Sigmundsson et al., 2015; Thordarson & Larsen, 2007). In central Ethiopia, this link, or the absence of it, between rhyolitic and basaltic volcanic products is still under debate (e.g., Fontijn et al., 2018; Giordano et al., 2014; Hutchison, Fusillo, et al., 2016; Hutchison, Pyle, et al., 2016). At Aluto, the two compositions seem to be spatially partitioned, with basaltic volcanism occurring along the East Ziway volcanic field and the Wonji fault belt and silicic volcanism occurring almost exclusively across the volcanic edifice of Aluto and surroundings (e.g., Fontijn et al., 2018; Hutchison, Pyle, et al., 2016). Nevertheless, it seems unlikely that there would be no spatial overlap between silicic and basaltic volcanism, especially in some MER volcanic systems other than Aluto (e.g., Tullu Moye, Boset-Baricha; Fontijn et al., 2018; Siegburg et al., 2018). Two event-tree configurations could be adopted to tackle these issues: (a) probability of location given eruption composition is the parameter of the event tree (Figure S1c) or (b) probability of eruption composition given location is the parameter of the event tree (e.g., Sobradelo & Martí, 2010). In the first case, different data sets may be used to compute vent-opening probabilities for the different magma compositions and normalization factors should be used to ensure that the following expressions hold true:  $\sum_i P(\text{vent}_i | \text{silicic eruption}) = P(\text{silicic eruption})$ ,  $\sum_i P(\text{vent}_i | \text{basaltic eruption}) = P(\text{basaltic eruption})$  and, importantly,  $\sum_i P(\text{vent}_i | \text{silicic OR basaltic eruption}) = 1$ , assuming that  $P(\text{silicic OR basaltic eruption}) = P(\text{eruption})$ . In the second case (b) above, a common data set could be used to assess  $P(\text{vent}_i | \text{eruption})$  but then  $P(\text{silicic} | \text{vent}_i)$  and  $P(\text{basaltic} | \text{vent}_i)$  should be estimated. We anticipate that this may become complicated, even if vent locations are grouped into sectors (e.g., Marzocchi et al., 2008; Sobradelo & Martí, 2010).

#### 5.3.2. Phreatic and Phreatomagmatic Explosive Activity

One recurrent issue encountered while designing the event tree models was the spatial and temporal occurrence of phreatic and phreatomagmatic explosive activity (see Text S1 and Figure S1). In the first version of the event tree (Figure S1a), the focus at the “Eruption” node was on being able to discern between eruptions generating phreatic explosions only, and eruptions that may start with phreatic and/or phreatomagmatic explosions but then evolve toward other main eruptive phenomenology (e.g., Eyjafjallajökull 2010, Dellino et al., 2012; Sinabung 2013–2018, Gunawan et al., 2019). Our final event tree incorporates the latter situation only. The occurrence of phreatic explosions only may be explored in future expansions of the event tree toward short-term forecasts (Constantinescu et al., 2016; Rouwet et al., 2014). The spatial likelihood of phreatic and phreatomagmatic activity was also greatly debated, given that Aluto has developed a mature hydrothermal system (e.g., Braddock et al., 2017; Hutchison et al., 2015; Hutchison, Biggs, et al., 2016; Wilks et al., 2017), and there are permanent sources of shallow groundwater and surficial water available nearby, for example, lakes Ziway and Langano (Benvenuti et al., 2002). In addition, the effect of the rainy

seasons (*belg*, February–May; and *kiremt*, June–September) at Aluto can lead to the formation of a temporary intra-caldera lake (Friedrick Samrock, pers. comm., Fig. 3.47 in Clarke, 2020). Thus, the seasonal patterns in rainfall imply transient changes in the spatial probability of phreatic and phreatomagmatic explosive activity. Given the current lack of detailed data to try modeling such complexities, we simplify our event tree modeling by making the probability of phreatomagmatic eruptions spatially equiprobable. Nevertheless, with further research into the spatio-temporal dynamics of the groundwater system at Aluto and using the presented event tree, it would be feasible to adopt a parameterization that accounted for spatial variations in the probability of phreatomagmatic activity (e.g., Lindsay et al., 2010; Sandri et al., 2012).

### 5.3.3. Eruption Size and Scenarios

In PVHA, and across the volcanological community, there is still great debate about what measures are most adequate to define the size of a given eruption. Here, we leave aside the fact that volcanic eruptions are multistaged events composed of many distinctive eruptive phases (e.g., Cassidy et al., 2018; Jenkins et al., 2007; Ogburn et al., 2015; Siebert et al., 2010). Data requirements to model this intraeruption aleatory variability are enormous, and clearly lacking at Aluto, as research in this area of PVHA is currently under development (e.g., Bebbington & Jenkins, 2019; Wolpert et al., 2018).

The VEI has been widely used as a metric for explosions and explosive eruptions (e.g., Connor et al., 2001; Global Volcanism Program, 2013; Marzocchi et al., 2004; Newhall & Hoblitt, 2002; Ogburn et al., 2015; Sobradelo & Martí, 2010), in part because of its versatility to be assigned from varied data sets and observations, including historical data (Newhall & Self, 1982). However, this versatility has also been a source of criticism toward the VEI scale, for example, because the different criteria used to assign a specific VEI to a given explosive eruption (e.g., erupted volume and eruption column height), may not correspond to the same VEI size for certain eruptions (e.g., Orsi et al., 2009; Pyle, 2015; Rougier et al., 2018). Nevertheless, if volume of erupted pyroclastic material is considered the highest weighted parameter to define the VEI (and pyroclastic material associated with any dome collapse PDCs is not included) problems can be minimized. An additional challenge is the degree of specificity of the eruption scenarios that, almost unavoidably, are behind the selection of eruption sizes at a particular volcanic system of interest (e.g., Neri et al., 2008; Newhall & Pallister, 2015; Sandri et al., 2014; Sobradelo & Martí, 2010; Tierz, Sandri, Costa, Sulpizio, et al., 2016; Tierz, Sandri, Costa, Zaccarelli, et al., 2016). This complication represented a particular issue at Aluto. On the one hand, the eruption scenarios (Figure 2; Clarke et al., 2019; Clarke, 2020) are the best representation of what to expect at the volcano. However, they can become too specific to be successfully handled with a model to quantify volcanic hazard such as the event tree. In other words, if the chosen eruptive scenarios are very specific, it may be difficult to assess whether their union set satisfies the “mutually exclusive-and-exhaustive” requirement, commonly applied to nodes describing the eruption size in event tree models (Marzocchi et al., 2004, 2008, 2010; Newhall & Hoblitt, 2002; Sobradelo et al., 2014). Similarly, if known events at the volcano of interest cannot be related to eruption size metrics that are applicable across volcanic systems (e.g., VEI or magnitude; Global Volcanism Program, 2013; Croweller et al., 2012), then comparisons with eruptions from other volcanoes and/or the use of analog volcanoes to estimate the probability of different eruption sizes (Figures 4 and 5) can become virtually impossible.

## 6. Conclusions

In this work, we build the first published event tree model to quantify volcanic hazard at an African volcano: Aluto, in central Ethiopia. The model both conceptualizes the functioning of the volcanic system and provides a quantitative framework for probabilistic volcanic hazard assessment at Aluto volcano. Hazard analyses of specific phenomena, such as tephra fallout or pyroclastic density currents, can strongly benefit from the existence of the presented event tree model. The parameterization of the event tree model attempts to incorporate different sources of information and data available for Aluto volcano, from past and recent research, and use them to estimate the aleatory variability and, importantly, the large epistemic uncertainty currently associated with PVHA at Aluto. Results indicate that the effect of this epistemic uncertainty is significant for the different volcanic events represented in the event tree. This is particularly relevant for the long-term probability of eruption, because the epistemic uncertainty in this node cascades down to all the other nodes in the event tree. Future research carried out at Aluto (e.g., geological fieldwork and dating) could help reduce the epistemic uncertainty without necessarily requiring a significant modification of the event tree structure. Moreover, the presented event tree model could be translated to other volcanic

### Acknowledgments

The research leading to these results has been supported by UK Natural Environment Research Council Rift Volcanism: Past, Present and Future (RiftVolc) project (grant NE/L013460/1) and Global Geological Risk Platform of the British Geological Survey NC-ODA grant NE/R000069/1: Geoscience for Sustainable Futures. We sincerely thank Chris Newhall, Sarah Ogburn and Elisabeth Gallant for their thorough and very insightful reviews, which helped us improve the clarity of the manuscript significantly. We are also grateful to the Associate Editor, Marie Edmonds, for her editorial handling and support. We wholeheartedly thank Amdemichael Zafu, Ermias Filfilu, Victoria Smith, and Samantha Engwell for sharing fieldwork with us; Solomon Getachew and Zelalem Mandefro for safely driving us across beautiful Ethiopia; Benjamin Marchant and Daniela Cuba for leading the statistical setup and implementation of the expert elicitation; Samantha Engwell and Teri McNamara for participating as experts in the elicitation; and Will Hutchison, Charlotte Vye-Brown, Getnet Mewa, Atalay Ayele, Alessandro Tadini, Laura Sandri, Susanna Jenkins, Elodie Macorps, Chris Newhall, David Pyle, and Jonathan Hunt for fruitful discussions concerning some of the topics covered in this manuscript. Karen Fontijn developed part of her work at the Department of Earth Sciences, University of Oxford, UK. PT, BC, and EC led the conceptualization and development of the event tree models, SL significantly contributed to their first versions and SL, EL, GY, and KF contributed to subsequent versions. BC, EC, KF, FD, and PT teamed up to gather field evidence of proximal deposits of volcanic eruptions at Aluto. BC, EC, and KF led the processing and interpretation of such deposits. KF and FD teamed up to gather field evidence of distal deposits of volcanic eruptions at Aluto. KF led the processing and interpretation of such deposits. JC led the volcanological setup of the expert elicitation. PT built the event tree model using MATLAB (MATLAB, 2012), performed the intermediate steps required for its parameterization and computed the results derived from the model. PT and BC prepared the figures and wrote the manuscript. EC, FD, EL, GY, KF, JC, YB, and SL significantly helped editing the manuscript at different stages of its development. All authors read and approved all versions of the manuscript.

systems across the Main Ethiopian Rift by slightly updating its structure and significantly modifying its parameterization to reflect the particularities of each volcanic system. Structured, objective, and reproducible approaches to identify sets of analog volcanoes (VOLCANS, Tierz et al., 2019) could play a key role in exploring preliminary parameterizations as demonstrated here. Finally, despite some anticipated general and rift-related challenges to building event tree models across the MER and East African Rift, we argue that there is great potential to use this type of models to carry out probabilistic volcanic hazard assessment at many other volcanic systems in the region. In parallel, fundamental hazard-focused data collection is needed at these volcanoes.

### Data Availability Statement

Data sets for this research are included in these papers (and their supplementary information files): Crummy et al. (2018), Fontijn et al. (2018), McNamara et al. (2018), Tierz et al. (2019), and Clarke (2020). All data computed using VOLCANS (Tierz et al., 2019) have been deposited at <https://www.bgs.ac.uk/services/ngdc> and can be discovered at <https://doi.org/10.5285/f46c19aa-535f-4631-a032-60a2fc825a42> and accessed online (<https://www.bgs.ac.uk/services/ngdc/accessions/index.html#item135505>).

### References

- Alfano, F., Bonadonna, C., Volentik, A. C. M., Connor, C. B., Watt, S. F. L., Pyle, D. M., & Connor, L. J. (2011). Tephra stratigraphy and eruptive volume of the May, 2008, Chaitén eruption, Chile. *Bulletin of Volcanology*, 73(5), 613–630.
- Aspinall, W., Auken, M., Hincks, T., Mahony, S., Nadim, F., Pooley, J., et al. (2011). Volcano hazard and exposure in GFDRR priority countries and risk mitigation measures, Volcano Risk Study, 100,800–100,806.
- Aspinall, W. P., Carniel, R., Jaquet, O., Woo, G., & Hincks, T. (2006). Using hidden multi-state Markov models with multi-parameter volcanic data to provide empirical evidence for alert level decision-support. *Journal of Volcanology and Geothermal Research*, 153(1–2), 112–124. <https://doi.org/10.1016/j.jvolgeores.2005.08.010>
- Aspinall, W. P., Loughlin, S. C., Michael, F. V., Miller, A. D., Norton, G. E., Rowley, K. C., et al. (2002). The Montserrat Volcano Observatory: Its evolution, organization, role and activities. *Geological Society, London, Memoirs*, 21(1), 71–91. <https://doi.org/10.1144/GSL.MEM.2002.021.01.04>
- Aspinall, W. P., Woo, G., Voight, B., & Baxter, P. J. (2003). Evidence-based volcanology: application to eruption crises. *Journal of Volcanology and Geothermal Research*, 128(1–3), 273–285. [https://doi.org/10.1016/s0377-0273\(03\)00260-9](https://doi.org/10.1016/s0377-0273(03)00260-9)
- Auken, M., Sparks, R., Siebert, L., Crosweiler, H., & Ewert, J. (2013). A statistical analysis of the global historical volcanic fatalities record. *Journal of Applied Volcanology*, 2(1), 24.
- Baasner, A., Schmidt, B. C., & Webb, S. L. (2013). Compositional dependence of the rheology of halogen (F, Cl) bearing aluminosilicate melts. *Chemical Geology*, 346, 172–183.
- Barberi, F., Santacroce, R., & Varet, J. (1974). Silicic peralkaline volcanic rocks of the Afar Depression (Ethiopia). *Bulletin Volcanologique*, 38(2), 755–790.
- Bartolini, S., Geyer, A., Marti, J., Pedrazzi, D., & Aguirre-Díaz, G. (2014). Volcanic hazard on Deception Island (South Shetland Islands, Antarctica). *Journal of Volcanology and Geothermal Research*, 285, 150–168.
- Bayarri, M. J., Berger, J. O., Calder, E. S., Dalbey, K., Lunagomez, S., Patra, A. K., et al. (2009). Using statistical and computer models to quantify volcanic hazards. *Technometrics*, 51(4), 402–413. <https://doi.org/10.1198/TECH.2009.08018>
- Bebbington, M. S. (2007). Identifying volcanic regimes using hidden Markov models. *Geophysical Journal International*, 171(2), 921–942.
- Bebbington, M. S. (2013). Assessing probabilistic forecasts of volcanic eruption onsets. *Bulletin of Volcanology*, 75(12), 783.
- Bebbington, M. S. (2014). Long-term forecasting of volcanic explosivity. *Geophysical Journal International*, 197(3), 1500–1515.
- Bebbington, M. S. (2015). Spatio-volumetric hazard estimation in the Auckland volcanic field. *Bulletin of Volcanology*, 77(5), 39.
- Bebbington, M. S., & Jenkins, S. F. (2019). Intra-eruption forecasting. *Bulletin of Volcanology*, 81(6), 34.
- Becerril, L., Bartolini, S., Sobradelo, R., Marti, J., Morales, J. M., & Galindo, I. (2014). Long-term volcanic hazard assessment on El Hierro (Canary Islands). *Natural Hazards and Earth System Sciences*, 14(7), 1853–1870.
- Bekele, Y. (2017). Exposure-based risk analysis of Aluto volcano, Unpublished CERG-C 2017 Memoire Dissertation, Specialisation certificate in geological and climate related risk, University of Geneva, Switzerland.
- Benvenuti, M., Carnicelli, S., Belluomini, G., Dainelli, N., di Grazia, S., Ferrari, G. A., et al. (2002). The Ziway-Shala lake basin (main Ethiopian rift, Ethiopia): A revision of basin evolution with special reference to the Late Quaternary. *Journal of African Earth Sciences*, 35(2), 247–269. [https://doi.org/10.1016/S0899-5362\(02\)00036-2](https://doi.org/10.1016/S0899-5362(02)00036-2)
- Bevilacqua, A., Bursik, M., Patra, A., Pitman, E. B., & Till, R. (2017). Bayesian construction of a long-term vent opening probability map in the Long Valley volcanic region (CA, USA). *Statistics in Volcanology*, 3(1), 1.
- Bevilacqua, A., Flandoli, F., Neri, A., Isaia, R., & Vitale, S. (2016). Temporal models for the episodic volcanism of Campi Flegrei caldera (Italy) with uncertainty quantification. *Journal of Geophysical Research: Solid Earth*, 121, 7821–7845. <https://doi.org/10.1002/2016JB013171>
- Bevilacqua, A., Isaia, R., Neri, A., Vitale, S., Aspinall, W. P., Bisson, M., et al. (2015). Quantifying volcanic hazard at Campi Flegrei caldera (Italy) with uncertainty assessment: 1. Vent opening maps. *Journal of Geophysical Research: Solid Earth*, 120, 2309–2329. <https://doi.org/10.1002/2014JB011175>
- Biass, S., Bonadonna, C., Connor, L. J., & Connor, C. B. (2016). TephraProb: A Matlab package for probabilistic hazard assessments of tephra fallout. *Journal of Applied Volcanology*, 5(1), 10.
- Biggs, J., Bastow, I. D., Keir, D., & Lewi, E. (2011). Pulses of deformation reveal frequently recurring shallow magmatic activity beneath the Main Ethiopian Rift. *Geochemistry, Geophysics, Geosystems*, 12, Q0AB10. <https://doi.org/10.1029/2011GC003662>
- Blong, R. J. (1984). *Volcanic hazards. A sourcebook on the effects of eruptions*. Orlando, FL, USA: Academic Press, Inc.

- Braddock, M., Biggs, J., Watson, I. M., Hutchison, W., Pyle, D. M., & Mather, T. A. (2017). Satellite observations of fumarole activity at Aluto volcano, Ethiopia: Implications for geothermal monitoring and volcanic hazard. *Journal of Volcanology and Geothermal Research*, *341*, 70–83.
- Brown, S. K., Jenkins, S. F., Sparks, R. S. J., Odbert, H., & Auken, M. R. (2017). Volcanic fatalities database: Analysis of volcanic threat with distance and victim classification. *Journal of Applied Volcanology*, *6*(1), 1–20.
- Cassidy, M., Manga, M., Cashman, K., & Bachmann, O. (2018). Controls on explosive-effusive volcanic eruption styles. *Nature Communications*, *9*(1), 1–16.
- Castro, J. M., Schipper, C. I., Mueller, S. P., Militzer, A. S., Amigo, A., Parejas, C. S., & Jacob, D. (2013). Storage and eruption of near-liquidus rhyolite magma at Cordón Caulle, Chile. *Bulletin of Volcanology*, *75*(4), 702.
- Central Statistical Agency (2007). *The 2007 Population and Housing Census of Ethiopia: Statistical Report for Oromiya Region; Part I: Population Size and Characteristics*. Addis Ababa (Ethiopia): Population Census Commission, Federal Democratic Republic of Ethiopia.
- Chorowicz, J. (2005). The east African rift system. *Journal of African Earth Sciences*, *43*(1–3), 379–410.
- Clarke, B. (2020). Post-caldera eruptions and pyroclastic density current hazard in the Main Ethiopian Rift. PhD thesis, University of Edinburgh (p. 329).
- Clarke, B., Calder, E. S., Dessalegn, F., Fontijn, K., Cortés, J. A., Naylor, M., et al. (2019). Fluidal pyroclasts reveal the intensity of peralkaline rhyolite pumice cone eruptions. *Nature Communications*, *10*(1), 1–10.
- Clarke, B., Tierz, P., Calder, E., & Yirgu, G. (2020). Probabilistic Volcanic Hazard Assessment for Pyroclastic Density Currents From Pumice Cone Eruptions at Aluto Volcano, Ethiopia. *Frontiers in Earth Science*, *8*(348). <http://dx.doi.org/10.3389/feart.2020.00348>
- Connor, C. B., Bebbington, M. S., & Marzocchi, W. (2015). Probabilistic volcanic hazard assessment. In H. Sigurdsson, et al. (Eds.), *The encyclopedia of volcanoes (Second Edi)* (pp. 897–910). San Diego, CA, USA: Academic Press.
- Connor, C. B., Connor, L. J., Germa, A., Richardson, J. A., Bebbington, M. S., Gallant, E., & Saballos, A. (2018). How to use kernel density estimation as a diagnostic and forecasting tool for distributed volcanic vents. *Statistics in Volcanology*, *4*(1), 3.
- Connor, C. B., & Hill, B. E. (1995). Three nonhomogeneous Poisson models for the probability of basaltic volcanism: Application to the Yucca Mountain region, Nevada. *Journal of Geophysical Research*, *100*(B6), 10,107–10,125.
- Connor, C. B., Hill, B. E., Winfrey, B., Franklin, N. M., & la Femina, P. C. (2001). Estimation of volcanic hazards from tephra fallout. *Natural Hazards Review*, *2*(1), 33–42.
- Connor, L. J., Connor, C. B., Meliksetian, K., & Savov, I. (2012). Probabilistic approach to modeling lava flow inundation: A lava flow hazard assessment for a nuclear facility in Armenia. *Journal of Applied Volcanology*, *1*(1), 3.
- Constantinescu, R., Robertson, R., Lindsay, J. M., Tonini, R., Sandri, L., Rouwet, D., et al. (2016). Application of the probabilistic model BET\_UNREST during a volcanic unrest simulation exercise in Dominica, Lesser Antilles. *Geochemistry, Geophysics, Geosystems*, *17*, 4438–4456. <https://doi.org/10.1002/2016GC006485>
- Corti, G. (2009). Continental rift evolution: From rift initiation to incipient break-up in the Main Ethiopian Rift, East Africa. *Earth-Science Reviews*, *96*(1–2), 1–53.
- Corti, G. (2012). Evolution and characteristics of continental rifting: Analog modeling-inspired view and comparison with examples from the East African Rift System. *Tectonophysics*, *522*, 1–33.
- Croweller, H. S., Arora, B., Brown, S. K., Cottrell, E., Deligne, N. I., Guerrero, N. O., et al. (2012). Global database on large magnitude explosive volcanic eruptions (LaMEVE). *Journal of Applied Volcanology*, *1*(1), 4. <https://doi.org/10.1186/2191-5040-1-4>
- Crummy, J., Marchant, B., Loughlin, S. C., Engwell, S. L., Tierz, P., Cuba, D. M., & Vye-Brown, C. (2018). Elicitation of frequency and magnitude of potential future explosive eruptions at Corbetti and Aluto volcanoes, Ethiopia, British Geological Survey Open File Report (OR/18/061), 27pp.
- Dakin, G., & Gibson, I. L. (1971). A preliminary account of Aluto, a pantelleritic volcano in the Main Ethiopian rift. *Addis Ababa University Geophysical Observatory Bulletin*, *13*, 110–114.
- Dellino, P., Gudmundsson, M. T., Larsen, G., Mele, D., Stevenson, J. A., Thordarson, T., & Zimanowski, B. (2012). Ash from the Eyjafjallajökull eruption (Iceland): Fragmentation processes and aerodynamic behavior. *Journal of Geophysical Research*, *117*, B00C04. <https://doi.org/10.1029/2011JB008726>
- Di Genova, D., Romano, C., Hess, K. U., Vona, A., Poe, B. T., Giordano, D., et al. (2013). The rheology of peralkaline rhyolites from Pantelleria Island. *Journal of Volcanology and Geothermal Research*, *249*, 201–216. <https://doi.org/10.1016/j.jvolgeores.2012.10.017>
- Di Paola, G. M. (1972). The Ethiopian Rift Valley (between 7°00' and 8°40' lat. North). *Bulletin Volcanologique*, *36*(4), 517–560.
- Dingwell, D. B., Hess, K.-U., & Romano, C. (1998). Extremely fluid behavior of hydrous peralkaline rhyolites. *Earth and Planetary Science Letters*, *158*(1–2), 31–38.
- Ebinger, C. (2005). Continental break-up: The East African perspective. *Astronomy & Geophysics*, *46*(2), 2–16.
- Engwell, S. L., Sparks, R. S. J., & Aspinall, W. P. (2013). Quantifying uncertainties in the measurement of tephra fall thickness. *Journal of Applied Volcanology*, *2*(1), 5.
- Field, L., Blundy, J., Brooker, R. A., Wright, T., & Yirgu, G. (2012). Magma storage conditions beneath Dabbahu Volcano (Ethiopia) constrained by petrology, seismicity and satellite geodesy. *Bulletin of Volcanology*, *74*(5), 981–1004.
- Fontijn, K., Ernst, G. G. J., Bonadonna, C., Elburg, M. A., Mbede, E., & Jacobs, P. (2011). The ~4-ka Rungwe pumice (South-Western Tanzania): A wind-still Plinian eruption. *Bulletin of Volcanology*, *73*(9), 1353–1368.
- Fontijn, K., Ernst, G. G. J., Elburg, M. A., Williamson, D., Abdallah, E., Kwelwa, S., et al. (2010). Holocene explosive eruptions in the Rungwe Volcanic Province, Tanzania. *Journal of Volcanology and Geothermal Research*, *196*(1–2), 91–110. <https://doi.org/10.1016/j.jvolgeores.2010.07.021>
- Fontijn, K., McNamara, K., Zafu Tadesse, A., Pyle, D. M., Dessalegn, F., Hutchison, W., et al. (2018). Contrasting styles of post-caldera volcanism along the Main Ethiopian Rift: Implications for contemporary volcanic hazards. *Journal of Volcanology and Geothermal Research*, *356*, 90–113. <https://doi.org/10.1016/j.jvolgeores.2018.02.001>
- Fontijn, K., Williamson, D., Mbede, E., & Ernst, G. G. J. (2012). The Rungwe volcanic province, Tanzania—A volcanological review. *Journal of African Earth Sciences*, *63*, 12–31.
- Giordano, F., D'Antonio, M., Civetta, L., Tonarini, S., Orsi, G., Ayalew, D., et al. (2014). Genesis and evolution of mafic and felsic magmas at Quaternary volcanoes within the Main Ethiopian Rift: Insights from Gedemsa and Fanta'Ale complexes. *Lithos*, *188*, 130–144. <https://doi.org/10.1016/j.lithos.2013.08.008>
- Gleeson, M. L. M., Stock, M. J., Pyle, D. M., Mather, T. A., Hutchison, W., Yirgu, G., & Wade, J. (2017). Constraining magma storage conditions at a restless volcano in the Main Ethiopian rift using phase equilibria models. *Journal of Volcanology and Geothermal Research*, *337*, 44–61.

- Global Volcanism Program (2013). Volcanoes of the world, v. 4.6.7. Venzke, E (ed.). Smithsonian Institution. Available at: <https://doi.org/10.5479/si.GVP.VOTW4-2013>
- Gunawan, H., Budianto, A., Prambada, O., McCausland, W., Pallister, J., & Iguchi, M. (2019). Overview of the eruptions of Sinabung Volcano, 2010 and 2013–present and details of the 2013 phreatomagmatic phase. *Journal of Volcanology and Geothermal Research*, 382, 103–119. <https://doi.org/10.1016/j.jvolgeores.2017.08.005>
- Hengsdijk, H., & Jansen, H. C. (2006). *Agricultural development in the Central Ethiopian Rift valley: A desk-study on water-related issues and knowledge to support a policy dialogue*. Wageningen, The Netherlands: Plant Research International B.V.
- Hess, K.-U., Dingweil, D. B., & Webb, S. L. (1995). The influence of excess alkalis on the viscosity of a haplogranitic melt. *American Mineralogist*, 80(3–4), 297–304.
- Hincks, T. K., Komorowski, J.-C., Sparks, S. R., & Aspinall, W. P. (2014). Retrospective analysis of uncertain eruption precursors at La Soufrière volcano, Guadeloupe, 1975–77: Volcanic hazard assessment using a Bayesian Belief Network approach. *Journal of Applied Volcanology*, 3(1), 1–26.
- Horwell, C. J., & Baxter, P. J. (2006). The respiratory health hazards of volcanic ash: A review for volcanic risk mitigation. *Bulletin of Volcanology*, 69(1), 1–24.
- Houghton, B., Wilson, C., & Weaver, S. D. (1985). Strombolian deposits at Mayor Island basaltic eruption styles displayed by a peralkaline rhyolitic volcano. *New Zealand Geological Survey Record*, 8, 42–51.
- Hunt, J. A., Mather, T. A., & Pyle, D. M. (2020). Morphological comparison of distributed volcanic fields in the Main Ethiopian Rift using high-resolution digital elevation models. *Journal of Volcanology and Geothermal Research*, 393, 106732. <https://doi.org/10.1016/j.jvolgeores.2019.106732>
- Hunt, J. A., Pyle, D. M., & Mather, T. A. (2019). The geomorphology, structure, and lava flow dynamics of peralkaline rift volcanoes from high-resolution digital elevation models. *Geochemistry, Geophysics, Geosystems*, 20, 1508–1538. <https://doi.org/10.1029/2018GC008085>
- Hutchison, W., Biggs, J., Mather, T. A., Pyle, D. M., Lewi, E., Yirgu, G., et al. (2016). Causes of unrest at silicic calderas in the East African Rift: New constraints from InSAR and soil-gas chemistry at Aluto volcano, Ethiopia. *Geochemistry, Geophysics, Geosystems*, 17, 3008–3030. <https://doi.org/10.1002/2016GC006395>
- Hutchison, W., Fusillo, R., Pyle, D. M., Mather, T. A., Blundy, J. D., Biggs, J., et al. (2016). A pulse of mid-Pleistocene rift volcanism in Ethiopia at the dawn of modern humans. *Nature Communications*, 7(1), 1–12.
- Hutchison, W., Mather, T. A., Pyle, D. M., Biggs, J., & Yirgu, G. (2015). Structural controls on fluid pathways in an active rift system: A case study of the Aluto volcanic complex. *Geosphere*, 11(3), 542–562.
- Hutchison, W., Mather, T. A., Pyle, D. M., Boyce, A. J., Gleeson, M. L. M., Yirgu, G., et al. (2018). The evolution of magma during continental rifting: New constraints from the isotopic and trace element signatures of silicic magmas from Ethiopian volcanoes. *Earth and Planetary Science Letters*, 489, 203–218. <https://doi.org/10.1016/j.epsl.2018.02.027>
- Hutchison, W., Pyle, D. M., Mather, T. A., Yirgu, G., Biggs, J., Cohen, B. E., et al. (2016). The eruptive history and magmatic evolution of Aluto volcano: New insights into silicic peralkaline volcanism in the Ethiopian rift. *Journal of Volcanology and Geothermal Research*, 328, 9–33. <https://doi.org/10.1016/j.jvolgeores.2016.09.010>
- Iddon, F., Jackson, C., Hutchison, W., Fontijn, K., Pyle, D. M., Mather, T. A., et al. (2019). Mixing and crystal scavenging in the Main Ethiopian Rift revealed by trace element systematics in feldspars and glasses. *Geochemistry, Geophysics, Geosystems*, 20, 230–259. <https://doi.org/10.1029/2018GC007836>
- Jenkins, S. F., Magill, C., McAneney, J., & Blong, R. (2012). Regional ash fall hazard I: A probabilistic assessment methodology. *Bulletin of Volcanology*, 74(7), 1699–1712.
- Jenkins, S. F., Magill, C. R., & McAneney, K. J. (2007). Multi-stage volcanic events: A statistical investigation. *Journal of Volcanology and Geothermal Research*, 161(4), 275–288.
- Jenkins, S. F., Mee, K., Engwell, S. L., Lark, M., & Loughlin, S. C. (2015). Development of National Disaster Risk Profiles for Sub-Saharan Africa Volcanic Risk. Volcanic Hazard Report, World Bank/Global Facility for Disaster Risk Reduction and Recovery, M4.
- Kebede, S., Mamo, T., & Abebe, T. (1985). Geological report and explanation to the geological map of Aluto-Langano geothermal area. *Ethiopian Institute of Geological Surveys*, Addis Ababa (p. 60).
- Kendall, J.-M., Stuart, G. W., Ebinger, C. J., Bastow, I. D., & Keir, D. (2005). Magma-assisted rifting in Ethiopia. *Nature*, 433(7022), 146–148. <https://doi.org/10.1038/nature03161>
- Keranen, K., & Klempere, S. L. (2008). Discontinuous and diachronous evolution of the Main Ethiopian rift: Implications for development of continental rifts. *Earth and Planetary Science Letters*, 265(1–2), 96–111.
- Koller, D., & Friedman, N. (2009). *Probabilistic graphical models: principles and techniques*. Cambridge, MA, USA: MIT press.
- Lahitte, P., Gillot, P.-Y., & Courtillot, V. (2003). Silicic central volcanoes as precursors to rift propagation: The Afar case. *Earth and Planetary Science Letters*, 207(1–4), 103–116.
- Lindsay, J., Marzocchi, W., Jolly, G., Constantinescu, R., Selva, J., & Sandri, L. (2010). Towards real-time eruption forecasting in the Auckland volcanic field: Application of BET\_EF during the New Zealand National Disaster Exercise “Ruaumoko”. *Bulletin of Volcanology*, 72, 185–204.
- Loughlin, S. C., Sparks, S., Brown, S. K., Vye-Brown, C., & Jenkins, S. F. (2015). *Global volcanic hazards and risk*. Cambridge, UK: Cambridge University Press.
- Mahood, G. A. (1984). Pyroclastic rocks and calderas associated with strongly peralkaline magmatism. *Journal of Geophysical Research*, 89(B10), 8540–8552.
- Martin-Jones, C. M., Lane, C. S., Pearce, N. J. G., Smith, V. C., Lamb, H. F., Schaebitz, F., et al. (2017). Recurrent explosive eruptions from a high-risk Main Ethiopian Rift volcano throughout the Holocene. *Geology*, 45(12), 1127–1130. <https://doi.org/10.1130/G39594.1>
- Marzocchi, W., & Bebbington, M. S. (2012). Probabilistic eruption forecasting at short and long time scales. *Bulletin of Volcanology*, 74(8), 1777–1805.
- Marzocchi, W., & Jordan, T. H. (2014). Testing for ontological errors in probabilistic forecasting models of natural systems. *Proceedings of the National Academy of Sciences*, 111(33), 11,973–11,978.
- Marzocchi, W., Newhall, C., & Woo, G. (2012). The scientific management of volcanic crises. *Journal of Volcanology and Geothermal Research*, 247, 181–189.
- Marzocchi, W., Sandri, L., Gasparini, P., Newhall, C., & Boschi, E. (2004). Quantifying probabilities of volcanic events: The example of volcanic hazard at Mount Vesuvius. *Journal of Geophysical Research*, 109, B11201. <https://doi.org/10.1029/2004JB003155>
- Marzocchi, W., Sandri, L., & Selva, J. (2008). BET\_EF: A probabilistic tool for long-and short-term eruption forecasting. *Bulletin of Volcanology*, 70(5), 623–632.

- Marzocchi, W., Sandri, L., & Selva, J. (2010). BET\_VH: A probabilistic tool for long-term volcanic hazard assessment. *Bulletin of Volcanology*, 72(6), 705–716.
- Marzocchi, W., & Woo, G. (2007). Probabilistic eruption forecasting and the call for an evacuation. *Geophysical Research Letters*, 34, L22310. <https://doi.org/10.1029/2007GL031922>
- Mastin, L. G., Guffanti, M., Servranckx, R., Webley, P., Barsotti, S., Dean, K., et al. (2009). A multidisciplinary effort to assign realistic source parameters to models of volcanic ash-cloud transport and dispersion during eruptions. *Journal of Volcanology and Geothermal Research*, 186(1–2), 10–21. <https://doi.org/10.1016/j.jvolgeores.2009.01.008>
- MATLAB (2012). *MATLAB release 2012B*. Natick, MA, United States: The MathWorks, Inc.
- McNamara, K., Cashman, K. V., Rust, A. C., Fontijn, K., Chalié, F., Tomlinson, E. L., & Yirgu, G. (2018). Using lake sediment cores to improve records of volcanism at Aluto volcano in the Main Ethiopian Rift. *Geochemistry, Geophysics, Geosystems*, 19, 3164–3188. <https://doi.org/10.1029/2018GC007686>
- Mohr, P. (1983). Volcanotectonic aspect of Ethiopian rift evolution. *Bulletin des Centres de Recherches Exploration-Production Elf-Aquitaine*, 7(1), 175–189.
- Monserrat Volcano Observatory, Baxter, P. J., Woo, G., & Pomonis, A. (1998). *Preliminary assessment of volcanic risk on Montserrat*. Montserrat, West Indies. Available at: Montserrat Volcano Observatory. <http://www.geo.mtu.edu/volcanoes/west.indies/soufriere/govt/miscdocs/prelimvolcrisk.html>
- Neri, A., Aspinall, W. P., Cioni, R., Bertagnini, A., Baxter, P. J., Zuccaro, G., et al. (2008). Developing an event tree for probabilistic hazard and risk assessment at Vesuvius. *Journal of Volcanology and Geothermal Research*, 178(3), 397–415. <https://doi.org/10.1016/j.jvolgeores.2008.05.014>
- Newhall, C. G., & Hoblitt, R. (2002). Constructing event trees for volcanic crises. *Bulletin of Volcanology*, 64(1), 3–20.
- Newhall, C. G., & Pallister, J. S. (2015). Using multiple data sets to populate probabilistic volcanic event trees. In P. Papale, et al. (Eds.), *Volcanic hazards, risks, and disasters* (pp. 202–232). Amsterdam, Netherlands: Elsevier B. V.
- Newhall, C. G., & Self, S. (1982). The volcanic explosivity index (VEI) an estimate of explosive magnitude for historical volcanism. *Journal of Geophysical Research*, 87(C2), 1231–1238.
- Newhall, C. G., Self, S., & Robock, A. (2018). Anticipating future volcanic explosivity index (VEI) 7 eruptions and their chilling impacts. *Geosphere*, 14(2), 572–603.
- Ogburn, S. E. (2012). Flowdat-mass flow database (v2.2). Retrieved from <https://vhub.org/groups/massflowdatabase>
- Ogburn, S. E., Loughlin, S. C., & Calder, E. S. (2015). The association of lava dome growth with major explosive activity (VEI ≥ 4): DomeHaz, a global dataset. *Bulletin of Volcanology*, 77(5), 40.
- Orsi, G., Di Vito, M. A., Selva, J., & Marzocchi, W. (2009). Long-term forecast of eruption style and size at Campi Flegrei caldera (Italy). *Earth and Planetary Science Letters*, 287(1), 265–276.
- Orsi, G., Ruvo, L., & Scarpati, C. (1989). The Serra della Fastuca Tephra at Pantelleria: Physical parameters for an explosive eruption of peralkaline magma. *Journal of Volcanology and Geothermal Research*, 39(1), 55–60.
- Papale, P. (2017). Rational volcanic hazard forecasts and the use of volcanic alert levels. *Journal of Applied Volcanology*, 6(1), 13.
- Papale, P. (2018). Global time-size distribution of volcanic eruptions on Earth. *Scientific Reports*, 8(1), 6838. <https://doi.org/10.1038/s41598-018-25286-y>
- Peccerillo, A., Barberio, M. R., Yirgu, G., Ayalew, D., Barbieri, M., & Wu, T. W. (2003). Relationships between mafic and peralkaline silicic magmatism in continental rift settings: A petrological, geochemical and isotopic study of the Gedemsa volcano, central Ethiopian rift. *Journal of Petrology*, 44(11), 2003–2032.
- Peccerillo, A., Donati, C., Santo, A. P., Orlando, A., Yirgu, G., & Ayalew, D. (2007). Petrogenesis of silicic peralkaline rocks in the Ethiopian rift: Geochemical evidence and volcanological implications. *Journal of African Earth Sciences*, 48(2–3), 161–173.
- Poland Michael P., & Anderson Kyle R. (2020). Partly Cloudy With a Chance of Lava Flows: Forecasting Volcanic Eruptions in the Twenty-First Century. *Journal of Geophysical Research: Solid Earth*, 125, e2018JB016974. <http://dx.doi.org/10.1029/2018JB016974>
- Pyle, D. M. (2015). Sizes of volcanic eruptions. In H. Sigurdsson, et al. (Eds.), *The encyclopedia of volcanoes (Second Edi)* (pp. 257–264). San Diego, CA, USA: Academic Press.
- Queiroz, G., Pacheco, J. M., Gaspar, J. L., Aspinall, W. P., Guest, J. E., & Ferreira, T. (2008). The last 5000 years of activity at Sete Cidades volcano (São Miguel Island, Azores): Implications for hazard assessment. *Journal of Volcanology and Geothermal Research*, 178(3), 562–573.
- Rappich, V., Žáček, V., Verner, K., Erban, V., Goslar, T., Bekele, Y., et al. (2016). Wendo Koshe Pumice: The latest Holocene silicic explosive eruption product of the Corbetti volcanic system (southern Ethiopia). *Journal of Volcanology and Geothermal Research*, 310, 159–171. <https://doi.org/10.1016/j.jvolgeores.2015.12.008>
- Riedel, C., Ernst, G. G. J., & Riley, M. (2003). Controls on the growth and geometry of pyroclastic constructs. *Journal of Volcanology and Geothermal Research*, 127(1–2), 121–152.
- Rooney, T. O., Hart, W. K., Hall, C. M., Ayalew, D., Ghiorsio, M. S., Hidalgo, P., & Yirgu, G. (2012). Peralkaline magma evolution and the tephra record in the Ethiopian Rift. *Contributions to Mineralogy and Petrology*, 164(3), 407–426.
- Rougier, J., Sparks, R. S. J., Cashman, K. V., & Brown, S. K. (2018). The global magnitude-frequency relationship for large explosive volcanic eruptions. *Earth and Planetary Science Letters*, 482, 621–629.
- Rougier, J., Sparks, R. S. J., & Hill, L. J. (2013). *Risk and uncertainty assessment for natural hazards*. Cambridge, UK: Cambridge University Press.
- Rouwet, D., Sandri, L., Marzocchi, W., Gottsmann, J., Selva, J., Tonini, R., & Papale, P. (2014). Recognizing and tracking volcanic hazards related to non-magmatic unrest: A review. *Journal of Applied Volcanology*, 3(1), 17.
- Rutarindwa, R., Spiller, E. T., Bevilacqua, A., Bursik, M. I., & Patra, A. K. (2019). Dynamic probabilistic hazard mapping in the Long Valley Volcanic Region CA: Integrating vent opening maps and statistical surrogates of physical models of pyroclastic density currents. *Journal of Geophysical Research: Solid Earth*, 124, 9600–9621. <https://doi.org/10.1029/2019JB017352>
- Rychert, C. A., Hammond, J. O. S., Harmon, N., Michael Kendall, J., Keir, D., Ebinger, C., et al. (2012). Volcanism in the Afar Rift sustained by decompression melting with minimal plume influence. *Nature Geoscience*, 5(6), 406–409. <https://doi.org/10.1038/ngeo1455>
- Sandri, L., Costa, A., Selva, J., Tonini, R., Macedonio, G., Folch, A., & Sulpizio, R. (2016). Beyond eruptive scenarios: Assessing tephra fallout hazard from Neapolitan volcanoes. *Scientific Reports*, 6(1), 1–13. <https://doi.org/10.1038/srep24271>
- Sandri, L., Guidoboni, E., Marzocchi, W., & Selva, J. (2009). Bayesian event tree for eruption forecasting (BET\_EF) at Vesuvius, Italy: A retrospective forward application to the 1631 eruption. *Bulletin of Volcanology*, 71(7), 729–745.

- Sandri, L., Jolly, G., Lindsay, J., Howe, T., & Marzocchi, W. (2012). Combining long-and short-term probabilistic volcanic hazard assessment with cost-benefit analysis to support decision making in a volcanic crisis from the Auckland Volcanic Field, New Zealand. *Bulletin of Volcanology*, *74*(3), 705–723.
- Sandri, L., Thouret, J.-C., Constantinescu, R., Biass, S., & Tonini, R. (2014). Long-term multi-hazard assessment for El Misti volcano (Peru). *Bulletin of Volcanology*, *76*(2), 1–26.
- Sandri, L., Tierz, P., Costa, A., & Marzocchi, W. (2018). Probabilistic hazard from pyroclastic density currents in the Neapolitan Area (Southern Italy). *Journal of Geophysical Research: Solid Earth*, *123*, 3474–3500. <https://doi.org/10.1002/2017JB014890>
- Selva, J., Costa, A., de Natale, G., di Vito, M. A., Isaia, R., & Macedonio, G. (2018). Sensitivity test and ensemble hazard assessment for tephra fallout at Campi Flegrei, Italy. *Journal of Volcanology and Geothermal Research*, *351*, 1–28.
- Selva, J., Costa, A., Marzocchi, W., & Sandri, L. (2010). BET\_VH: Exploring the influence of natural uncertainties on long-term hazard from tephra fallout at Campi Flegrei (Italy). *Bulletin of Volcanology*, *72*(6), 717–733.
- Selva, J., Costa, A., Sandri, L., Macedonio, G., & Marzocchi, W. (2014). Probabilistic short-term volcanic hazard in phases of unrest: A case study for tephra fallout. *Journal of Geophysical Research: Solid Earth*, *119*, 8805–8826. <https://doi.org/10.1002/2014JB011252>
- Selva, J., Marzocchi, W., Papale, P., & Sandri, L. (2012). Operational eruption forecasting at high-risk volcanoes: The case of Campi Flegrei, Naples. *Journal of Applied Volcanology*, *1*(1), 5. <https://doi.org/10.1186/2191-5040-1-5>
- Selva, J., Orsi, G., Di Vito, M. A., Marzocchi, W., & Sandri, L. (2012). Probability hazard map for future vent opening at the Campi Flegrei caldera, Italy. *Bulletin of Volcanology*, *74*(2), 497–510.
- Sheldrake, T. E., Sparks, R. S. J., Cashman, K. V., Wadge, G., & Aspinall, W. P. (2016). Similarities and differences in the historical records of lava dome-building volcanoes: Implications for understanding magmatic processes and eruption forecasting. *Earth-Science Reviews*, *160*, 240–263. <https://doi.org/10.1016/j.earscirev.2016.07.013>
- Siebert, L., Simkin, T., & Kimberly, P. (2010). *Volcanoes of the world (Third Edn)*. Berkeley, CA, USA: Univ of California Press.
- Sieburg, M., Gernon, T. M., Bull, J. M., Keir, D., Barfod, D. N., Taylor, R. N., et al. (2018). Geological evolution of the Boset-Bericha volcanic complex, Main Ethiopian Rift:  $^{40}\text{Ar}/^{39}\text{Ar}$  evidence for episodic Pleistocene to Holocene volcanism. *Journal of Volcanology and Geothermal Research*, *351*, 115–133. <https://doi.org/10.1016/j.jvolgeores.2017.12.014>
- Sigmundsson, F., Hooper, A., Hreinsdóttir, S., Vogfjörð, K. S., Ófeigsson, B. G., Heimisson, E. R., et al. (2015). Segmented lateral dyke growth in a rifting event at Bárðarbunga volcanic system, Iceland. *Nature*, *517*(7533), 191–195. <https://doi.org/10.1038/nature14111>
- Sobradelo, R., Bartolini, S., & Marti, J. (2014). HASSET: A probability event tree tool to evaluate future volcanic scenarios using Bayesian inference. *Bulletin of Volcanology*, *76*(1), 770.
- Sobradelo, R., & Marti, J. (2010). Bayesian event tree for long-term volcanic hazard assessment: Application to Teide-Pico Viejo strato-volcanoes, Tenerife, Canary Islands. *Journal of Geophysical Research*, *115*, B05206. <https://doi.org/10.1029/2009JB006566>
- Spiller, E. T., Bayarri, M. J., Berger, J. O., Calder, E. S., Patra, A. K., Pitman, E. B., & Wolpert, R. L. (2014). Automating emulator construction for geophysical hazard maps. *SIAM/ASA Journal on Uncertainty Quantification*, *2*(1), 126–152.
- Stefanescu, E. R., Bursik, M., Cordoba, G., Dalbey, K., Jones, M. D., Patra, A. K., et al. (2012). Digital elevation model uncertainty and hazard analysis using a geophysical flow model. *Proceedings of the Royal Society A: Mathematical, Physical and Engineering Science*, *468*(2142), 1543–1563. <https://doi.org/10.1098/rspa.2011.0711>
- Thordarson, T., & Larsen, G. (2007). Volcanism in Iceland in historical time: Volcano types, eruption styles and eruptive history. *Journal of Geodynamics*, *43*(1), 118–152.
- Tierz, P. (2020). Long-term probabilistic volcanic hazard assessment using open and non-open data: Observations and current issues. *Frontiers in Earth Science*, *8*, 257. <https://doi.org/10.3389/feart.2020.00257>
- Tierz, P., Loughlin, S. C., & Calder, E. S. (2019). VOLCANS: An objective, structured, reproducible method for identifying sets of analogue volcanoes. *Bulletin of Volcanology*, *81*(12), 1–22. <https://doi.org/10.1007/s00445-019-1336-3>
- Tierz, P., Sandri, L., Costa, A., Sulpizio, R., Zaccarelli, L., Vito, M. A. D., & Marzocchi, W. (2016). Uncertainty assessment of pyroclastic density currents at Mount Vesuvius (Italy) simulated through the energy cone model. In K. Riley, et al. (Eds.), *Natural hazard uncertainty assessment: Modeling and decision support, AGU geophysical monograph series 223* (pp. 125–145). Hoboken, NJ, USA: John Wiley & Sons, Inc. <https://doi.org/10.1002/9781119028116.ch9>
- Tierz, P., Sandri, L., Costa, A., Zaccarelli, L., di Vito, M. A., Sulpizio, R., & Marzocchi, W. (2016). Suitability of energy cone for probabilistic volcanic hazard assessment: Validation tests at Somma-Vesuvius and Campi Flegrei (Italy). *Bulletin of Volcanology*, *78*(11), 1–15. <https://doi.org/10.1007/s00445-016-1073-9>
- Tierz, P., Stefanescu, E. R., Sandri, L., Sulpizio, R., Valentine, G. A., Marzocchi, W., & Patra, A. K. (2018). Towards quantitative volcanic risk of pyroclastic density currents: Probabilistic hazard curves and maps around Somma-Vesuvius (Italy). *Journal of Geophysical Research: Solid Earth*, *123*, 6299–6317. <https://doi.org/10.1029/2017JB015383>
- Tierz, P., Woodhouse, M. J., Phillips, J. C., Sandri, L., Selva, J., Marzocchi, W., & Odbert, H. M. (2017). A framework for probabilistic multi-hazard assessment of rain-triggered lahars using Bayesian belief networks. *Frontiers in Earth Science*, *5*, 73. <https://doi.org/10.3389/feart.2017.00073>
- Tonini, R., Sandri, L., & Thompson, M. A. (2015). PyBetVH: A Python tool for probabilistic volcanic hazard assessment and for generation of Bayesian hazard curves and maps. *Computers & Geosciences*, *79*, 38–46.
- United Nations Development Programme. (2018). Human development reports - Ethiopia.
- Vye-Brown, C., Sparks, R. S. J., Lewi, E., Mewa, G., Asrat, A., Loughlin, S. C., et al. (2016). Ethiopian volcanic hazards: A changing research landscape. *Geological Society, London, Special Publications*, *420*(1), 355–365. <https://doi.org/10.1144/SP420.16>
- Wadge, G., Biggs, J., Lloyd, R., & Kendall, J.-M. (2016). Historical volcanism and the state of stress in the east African rift system. *Frontiers in Earth Science*, *4*, 86.
- Wadge, G., Voight, B., Sparks, R. S. J., Cole, P. D., Loughlin, S. C., & Robertson, R. E. A. (2014). An overview of the eruption of Soufrière Hills volcano, Montserrat from 2000 to 2010. *Geological Society, London, Memoirs*, *39*(1), 1–40.
- Weller, J. N., Martin, A. J., Connor, C. B., Connor, L. J., & Karakhanian, A. (2006). Modelling the spatial distribution of volcanoes: An example from Armenia. In H. M. Mader, et al. (Eds.), *Statistics in volcanology, Special Publications of IAVCEI, 1* (pp. 77–88). London, UK: the geological society.
- Wetmore, P. H., Hughes, S. S., Connor, L. J., & Caplinger, M. L. (2009). Spatial distribution of eruptive centers about the Idaho National Laboratory. In C. B. Connor, et al. (Eds.), *Volcanic and Tectonic Hazard Assessment for Nuclear Facilities* (pp. 385–405, 229256). Cambridge, UK: Cambridge University press.
- Wilks, M., Kendall, J. M., Nowacki, A., Biggs, J., Wookey, J., Birhanu, Y., et al. (2017). Seismicity associated with magmatism, faulting and hydrothermal circulation at Aluto volcano, Main Ethiopian Rift. *Journal of Volcanology and Geothermal Research*, *340*, 52–67. <https://doi.org/10.1016/j.jvolgeores.2017.04.003>

- Wilson, T. M., Stewart, C., Sword-Daniels, V., Leonard, G. S., Johnston, D. M., Cole, J. W., et al. (2012). Volcanic ash impacts on critical infrastructure. *Physics and Chemistry of the Earth, Parts A/B/C*, *45*, 5–23.
- Woldegabriel, G., Aronson, J. L., & Walter, R. C. (1990). Geology, geochronology, and rift basin development in the central sector of the Main Ethiopia Rift. *Geological Society of America Bulletin*, *102*(4), 439–458.
- Wolpert, R. L., Spiller, E. T., & Calder, E. S. (2018). Dynamic statistical models for pyroclastic density current generation at Soufrière Hills volcano. *Frontiers in Earth Science*, *6*, 55. <https://doi.org/10.3389/feart.2018.00055>
- Woo, G. (1999). *The mathematics of natural catastrophes*. London, UK: Imperial College Press.
- Woodhouse, M. J., Hogg, A. J., Phillips, J. C., & Sparks, R. S. J. (2013). Interaction between volcanic plumes and wind during the 2010 Eyjafjallajökull eruption, Iceland. *Journal of Geophysical Research: Solid Earth*, *118*, 92–109. <https://doi.org/10.1029/2012JB009592>
- World Bank, World Development Indicators (2019). Population, total [Ethiopia]. Retrieved from <https://data.worldbank.org/country/ethiopia?view=chart>
- Wright, H. M. N., Pallister, J. S., McCausland, W. A., Griswold, J. P., Andreastuti, S., Budianto, A., et al. (2019). Construction of probabilistic event trees for eruption forecasting at Sinabung volcano, Indonesia 2013–14. *Journal of Volcanology and Geothermal Research*, *382*, 233–252. <https://doi.org/10.1016/j.jvolgeores.2018.02.003>
- Yirgu, G., Ferguson, D. J., Barnie, T. D., & Oppenheimer, C. (2014). Recent volcanic eruptions in the Afar rift, northeastern Africa, and implications for volcanic risk management in the region. In A. Ismail-Zadeh, et al. (Eds.), *Extreme natural hazards, disaster risks and societal implications* (pp. 200–213). Cambridge: Cambridge University Press.

## References From the Supporting Information

- Barberi, F., Bertagnini, A., Landi, P., & Principe, C. (1992). A review on phreatic eruptions and their precursors. *Journal of Volcanology and Geothermal Research*, *52*(4), 231–246. [https://doi.org/10.1016/0377-0273\(92\)90046-G](https://doi.org/10.1016/0377-0273(92)90046-G)
- Cannavò, F., Cannata, A., Cassisi, C., di Grazia, G., Montalto, P., Prestifilippo, M., et al. (2017). A multivariate probabilistic graphical model for real-time volcano monitoring on Mount Etna. *Journal of Geophysical Research: Solid Earth*, *122*, 3480–3496. <https://doi.org/10.1002/2016JB013512>
- Christiansen, R. L., Lowenstern, J. B., Smith, R. B., Heasler, H., Morgan, L. A., Nathenson, M., et al. (2007). Preliminary assessment of volcanic and hydrothermal hazards in Yellowstone National Park and vicinity, U.S. Geol. Surv. Open-File Rep., 71, 94.
- Christophersen, A., Deligne, N. I., Hanea, A. M., Chardot, L., Fournier, N., & Aspinall, W. P. (2018). Bayesian network modeling and expert elicitation for probabilistic eruption forecasting: Pilot study for Whakaari/White Island, New Zealand. *Frontiers in Earth Science*, *6*, 211.
- Houghton, B., White, J. D. L., & Van Eaton, A. R. (2015). Phreatomagmatic and related eruption styles. In H. Sigurdsson, et al. (Eds.), *The encyclopedia of volcanoes (Second Edi)* (pp. 537–552). San Diego, CA, USA: Academic Press.
- Neri, A., Bevilacqua, A., Esposti Ongaro, T., Isaia, R., Aspinall, W. P., Bisson, M., et al. (2015). Quantifying volcanic hazard at Campi Flegrei caldera (Italy) with uncertainty assessment: 2. Pyroclastic density current invasion maps. *Journal of Geophysical Research: Solid Earth*, *120*, 2330–2349. <https://doi.org/10.1002/2014JB011776>
- Strehlow, K., Sandri, L., Gottsmann, J. H., Kilgour, G., Rust, A. C., & Tonini, R. (2017). Phreatic eruptions at crater lakes: Occurrence statistics and probabilistic hazard forecast. *Journal of Applied Volcanology*, *6*(1), 4.
- Thompson, M. A., Lindsay, J. M., Sandri, L., Biass, S., Bonadonna, C., Jolly, G., & Marzocchi, W. (2015). Exploring the influence of vent location and eruption style on tephra fall hazard from the Okataina Volcanic Centre, New Zealand. *Bulletin of Volcanology*, *77*(5), 38.